Imperial College London
Department of Theoretical Physics

New Examples of $\mathcal{PT}$-Symmetry Breaking For Quantum Systems

James McHugh

September 2009

Supervised by Carl M. Bender

Submitted in part fulfilment of the requirements for the degree of
Masters of Science in Theoretical Physics of Imperial College London
and the Diploma of Imperial College London

For John McClane.

"I am so clever that sometimes I don't understand a single word of what I am saying." - Oscar Wilde

Acknowledgements I would like to thank D.W. Hook for many useful discussions and P. Gorman, J. Marcq and M. Delph for many useless discussions.

Abstract

An overview of the theory of $\mathcal{PT}$-symmetric quantum mechanics and some of its applications and consequence is provided. The classical counterpart of $\mathcal{PT}$-symmetric quantum theories is discussed, with the novel classical phenomenon of spontaneous $\mathcal{PT}$- symmetry breaking highlighted.

A Runge-Kutta routine is developed to examine the spectrum of quantum Hamiltonians. This routine is then extended and applied to a class of $\mathcal{PT}$ -symmetric Hamiltonians, reproducing an already known result. The routine is ultimately applied to the quantum equivalent of the classical systems which exhibit spontaneous $\mathcal{PT}$- symmetry breaking, and a quantum counterpart to this phenomenon is observed.

Contents

1 Introduction

The study of $\mathcal{PT}$-symmetric quantum mechanics originates from the study of the eigenspectrum of the Hamiltonian $H = \hat{p}^2 + i\hat{x}^2 + ig\hat{h}^3$. This Hamiltonian arises in the context of the Yang-Lee edge singularity [1] [2] [3]. In the strong-coupling limit this Hamiltonian becomes

$$H = \hat{p}^2 + i\hat{x}^3 \tag{1.1}$$

Some early numerical work by Bessis and Zinn-Justin in 1993 had indicated that a portion of the eigenvalue spectrum for this Hamiltonian was real. It was then speculated that the spectrum might be entirely real,

In 1998 it was discovered by Bender and Boettcher that this was the case, that the spectrum of 1.1 was real, and that the aforementioned Hamiltonian was but one of an entire family of non-Hermitian Hamiltonians displaying a real eigenvalue spectrum. [4]

$$H = \hat{p}^2 + x^2(ix)^\epsilon \tag{1.2}$$

For $\epsilon = 1$ this expression becomes equation 1.1.

It was argued that the reality of the eigenspectra of these Hamiltonians was a direct result of their symmetry under the $\mathcal{PT}$ operator, representing space-time reflections of the sysem, and that the condition of $\mathcal{PT}$ symmetry could replace the requirement that a Hamiltonian be Dirac Hermitian.

This requirement may be seen as desirable as it is more physically transparent than the traditional property of Hermiticity, which is an entirely mathematical constraint. This also brings to light the possibility of new theories which were previously thought to be unphysical in the Hermitian formulation of quantum mechanics, as it was thought that a non-Hermitian Hamiltonian would give rise to complex energy levels and a non-unitary time evolution. We will see that this is not the case if we make suitable modifications to our theory. Due to this many Hamiltonians which had pre-

viously been disregarded have become an avenue for the investigation for novel new theories. [5]

The structure of this dissertation is as follows. In chapter 2 we will provide a brief overview of the development and chief properties of $\mathcal{PT}$ symmetric quantum mechanics, some of its potential applications.

In chapter 3 we discuss the classical counterparts of $\mathcal{PT}$ symmetric quantum theories, these are the classical motion of a particle in the complex plane subject to the complex force law of a $\mathcal{PT}$-symmetric Hamiltonian. In chapter 4 we begin to develop the numerical techniques which may be employed to examine the spectra of classes of $\mathcal{PT}$-symmetric Hamiltonians.

In chapter 5 an unusual set of behaviours for the classical systems reviewed in 3 is discussed. The correspondence between the classical and quantum regimes is explored, on the basis of which it is decided to apply the numerical techniques developed in 4 in the previously unexamined quantum scenario. In chapter 6 the previously observed numerical result for the class of Hamiltonians we are observing is reproduced, and the behaviour of other $\mathcal{PT}$-symmetric Hamiltonians is reviewed. In chapter 7 these techniques are applied to the quantum analogue of the phenomena outlined in chapter 5, the results of which are detailed and commented upon.

Finally, in chapter 8 we comment upon our results and indicate some potentially fruitful avenues for future investigation.

2 $\mathcal{PT}$ Symmetric Quantum Mechanics

2.1 The Hamiltonian in Quantum Mechanics

Since this subject relies heavily on the role of the Hamiltonian, and on the extension of the normal properties assumed of a Hamiltonian, we will first give a short discussion of the role that is played by the Hamiltonian in traditional quantum mechanics, and on some other aspects of quantum mechanics.

In traditional textbook quantum mechanics, the Hamiltonian plays three vital roles in our theory: it specifies the spectrum of energy eigenvalues which the theory may possess, it defines the time evolution of the system, and it enumerates the symmetries of the theory through its commutation relations with the various operators associated to those symmetries. We give a brief overview of these properties in this section.

The *time-dependent Schrodinger equation* stipulates that

$$-i\hbar\frac{\partial|\psi\rangle}{\partial t} = \hat{H}|\psi\rangle$$

And it follows that

$$\psi(t) = \psi(t_0)e^{-iHt}$$

From which we can deduce the form of the time evolution operator, U(t)

$$U(t) = e^{-i\hat{H}t}$$

As ever, the probability of getting a certain result for a measurement is associated with a particular operator. The eigenvectors of these operators span the Hilbert space of the system. When we perform a measurement upon the system we will measure it to be in a state with the eigenvalue

associated to a certain eigenvector with probability $\propto \langle e_i|e_i\rangle$, where $|e_i\rangle$ is the eigenvector associated with the eigenvalue i, and by $\langle|\rangle$ we refer to a map from the Hilbert Space and it's dual space into the real numbers.s

As the eigenvectors span the Hilbert space, we can write any state as a linear combination of them. If we normalise our state we require that $\langle\psi|\psi\rangle = 1$, that is, that the total probability of measuring the state to be in *any* eigenstate is equal to one. We can then reason that the time evolution of our system must be unitary. [6] [7] That is,

$$U(t)U^\dagger(t) = \mathbb{I} \tag{2.1}$$

where by $U^\dagger$ we mean ordinary Hermitian conjugation. That is, we take the complex conjugate of the components of the matrix of the operator represented in some basis and then transpose the resulting matrix. If the operator U is unitary then the absolute value of the state vector is preserved under time evolution, and so probability is conserved.

In traditional quantum mechanics we stipulate that the Hamiltonian be Hermitian as an axiom of the theory. If we require this property of our theory, we can guarantee that we have unitary time evolution of the states of the system as well as an entirely real spectrum for the energy eigenstates.

We can see that unitary time evolution follows as

$$U(t)U^\dagger(t) = e^{-iHt_0}e^{iH^\dagger t_0} = e^{-i(H-H^\dagger)t_0} = \mathbb{I} \tag{2.2}$$

and since we have required that $H = H^\dagger$ the product of U and $U^\dagger$ is the identity.

Finally, as the Hamiltonian operator defines the time evolution of the system any operation under which the system is invariant will commute with the Hamiltonian.

2.2 The $\mathcal{PT}$ operator.

Before defining $\mathcal{PT}$ symmetry, we must first discuss how the $\mathcal{P}$ and $\mathcal{T}$ operators will act on the Hilbert space of a quantum theory.

2.2.1 Properties of the $\mathcal{P}$ and $\mathcal{T}$ operators

The *parity* and *time-reversal* operators are discrete orthogonal transformations. These transformations are not rotations, that is, the determinant of the operators is -1 - in other words, they describe reflections of our coordinate systems. From this statement we can immediately deduce that

$$\mathcal{P}^2 = \mathcal{T}^2 = \mathbb{I}$$

The parity operator $\mathcal{P}$ maps a spatial 3-vector $\vec{x}$ to $-\vec{x}$, It follows that both the position vector, $\vec{x}$ and the momentum vector, $\vec{p}$, are negated, as momentum is the mass times the time derivative of the position.

In a quantum mechanical system, the position and momentum are represented by operators:

$$\hat{p}|\psi\rangle = p|\psi\rangle \quad \text{and} \quad \hat{x}|\psi\rangle = x|\psi\rangle$$

Where $\hat{x}$ and $\hat{p}$ represent operators on the Hilbert space of the system and x and p respresent their respective eigenvalues. Given the classical behaviour of the $\mathcal{P}$ operator we expect that upon applying a parity transformation to our Hilbert space, the eigenvalues of the respective operators will be negated. So, we apply $\mathcal{P}$ to the system, and the operators and vectors are changed as follows.

$$\begin{aligned} |\psi\rangle &\rightarrow \mathcal{P}|\psi\rangle = |\psi'\rangle \\ \hat{x} &\rightarrow \mathcal{P}\hat{x}\mathcal{P} = \hat{x'} \\ \hat{p} &\rightarrow \mathcal{P}\hat{p}\mathcal{P} = \hat{p'} \end{aligned}$$

To reproduce the classical behaviour we expect that

$$\hat{x'}|\psi'\rangle = -x|\psi'\rangle$$

From which we can deduce that under the $\mathcal{P}$ transformation, the $\hat{x}$ operator becomes $\hat{x}' = \mathcal{P}\hat{x}\mathcal{P} = -\hat{x}$

$$\begin{aligned} (\mathcal{P}\hat{x}\mathcal{P})\mathcal{P}|\psi\rangle &= -\mathcal{P}\hat{x}\mathcal{P}^2|\psi\rangle \\ &= -\mathcal{P}\hat{x}\mathbb{I}|\psi\rangle \\ &= -\mathcal{P}x|\psi\rangle \\ &= -x|\psi'\rangle \end{aligned}$$

So we can see that we can only get the sort of behaviour we expect if $\hat{x}$ and $\hat{p}$ transform in the following way

$$\begin{aligned}\mathcal{P}\hat{x}\mathcal{P} &= -\hat{x} \\ \mathcal{P}\hat{p}\mathcal{P} &= -\hat{p}\end{aligned}$$

Similary, the $\mathcal{T}$ transformation classically maps the time t to -t. $\vec{x}$ is then mapped to $\vec{x}$, and $\vec{p}$ is mapped to $-\vec{p}$, as $\vec{p}$ is the time derivative of the position vector. This leads us to conclude that $\hat{x}$ and $\hat{p}$ transform as follows

$$\begin{aligned}\mathcal{T}\hat{x}\mathcal{T} &= \hat{x} \\ \mathcal{T}\hat{p}\mathcal{T} &= -\hat{p}\end{aligned}$$

However, there is one important caveat here! The quantum theory must remain invariant under these transformations. In particular, the commutation relation for the $\hat{p}$ and $\hat{x}$ operators must be invariant. After all, we have only specified a change of coordinates here, so the relationship between $\hat{x}$ and $\hat{p}$ operators must remain the same.

The commutation relation demands that

$$[\hat{x}, \hat{p}] = -i\hbar\mathbb{I}$$

After the $\mathcal{T}$ transformation this becomes:

$$\begin{aligned}[\hat{x'}, \hat{p'}] &= [\mathcal{T}\hat{x}\mathcal{T}, \mathcal{T}\hat{p}\mathcal{T}] \\ &= (\mathcal{T}\hat{x}\mathcal{T})(\mathcal{T}\hat{p}\mathcal{T}) - (\mathcal{T}\hat{p}\mathcal{T})(\mathcal{T}\hat{x}\mathcal{T}) \\ &= -\hat{x}\hat{p} + \hat{p}\hat{x} \\ &= -[\hat{x}, \hat{p}] = i\hbar\mathbb{I}\end{aligned}$$

So in order to preserve the commutation relations we demand that under the $\mathcal{T}$ transformation i $\rightarrow$ -i. When this is the case we say that the $\mathcal{T}$ operator is *antilinear*.

In short, we see that $\mathcal{P}$ is linear and inverts the sign of the $\hat{x}$ and $\hat{p}$ operators. $\mathcal{T}$ is anti-linear, reversing the sign of the $\hat{p}$ operator and performing complex conjugation. [8]

The behaviour of the $\mathcal{PT}$ operator may be arrived at from iterated application of the above rules.

$$\begin{aligned}\mathcal{PT}\hat{x}\mathcal{PT} &= -\hat{x} \\ \mathcal{PT}\hat{p}\mathcal{PT} &= \hat{p}\end{aligned}$$

We can also see that the $\mathcal{P}$ and $\mathcal{T}$ operators must commute with each other. because they implement reflections of orthogonal coordinates.

$$[\mathcal{P}, \mathcal{T}] = 0$$

2.2.2 $\mathcal{PT}$ symmetry.

In order to discuss $\mathcal{PT}$ symmetric quantum theories, we must first define the notion of $\mathcal{PT}$ symmetry. In analogy to the case of Dirac Hermiticity, we define a $\mathcal{PT}$ symmetric Hamiltonian as one which satisfies:

$$H = H^{\mathcal{PT}} \tag{2.3}$$

Where $H^{\mathcal{PT}} = (\mathcal{PT})H(\mathcal{PT})$. That is, when we apply the $\mathcal{P}$ and $\mathcal{T}$ transformations to the Hilbert space, the Hamiltonian is unchanged.

The condition that $H = H^{\mathcal{PT}}$ also implies that the H operator commutes with the $\mathcal{PT}$ operator. Given that $(\mathcal{PT})^{-1} = \mathcal{PT}$,

$$\begin{aligned}H &= (\mathcal{PT})H(\mathcal{PT}) \\ H\mathcal{PT} &= \mathcal{PT}H \\ H\mathcal{PT} - \mathcal{PT}H &= 0\end{aligned}$$

So we see that $[H, \mathcal{PT}] = 0$.

2.3 Reality of Eigenvalues

Having defined the notion of a $\mathcal{PT}$ symmetric Hamiltonian we will now show what this condition implies for the the eigenvalue spectrum of a Hamiltonian which obeys this symmetry.

First we will show that the eigenvalues of the $\mathcal{PT}$ operator have a modulus equal to one and hence are phase factors. We act upon the state ψ with the $\mathcal{PT}$ operator

$$\mathcal{PT}\psi = \lambda\psi$$

This gives us some unspecified eigenvalue which is in principle complex. Using the fact that $(\mathcal{PT})^2 = \mathbb{I}$ and that $[\mathcal{P}, \mathcal{T}] = 0$

$$(\mathcal{PT})(\mathcal{PT})\psi = (\mathcal{PT})\lambda\psi = \psi$$

inserting $(\mathcal{PT})^2$:

$$\begin{aligned} \psi &= \mathcal{PT}\lambda(\mathcal{PT})^2\psi \\ \psi &= (\mathcal{PT})\lambda(\mathcal{PT})(\mathcal{PT}\psi) \\ \psi &= (\mathcal{PT}\lambda\mathcal{PT})(\mathcal{PT})\psi \end{aligned}$$

And so we see that

$$\lambda^*\mathcal{PT}\psi = \lambda^*\lambda\psi = |\lambda|^2\psi$$

That is

$$\psi = |\lambda|^2\psi$$

We may therefore deduce that $|\lambda|^2 = 1$ and hence that $\lambda = e^{i\theta}$.
Referring to the Schrodinger equation

$$H\psi = E\psi$$

Inserting $(\mathcal{PT})^2$ and applying the $\mathcal{PT}$ operator

$$\begin{aligned} (\mathcal{PT})H\psi &= (\mathcal{PT})E(\mathcal{PT})^2\psi \\ H\mathcal{PT}\psi &= H\lambda\psi \\ H\lambda\psi &= (\mathcal{PT}E\mathcal{PT})(\mathcal{PT}\psi) \\ \lambda(H\psi) &= \lambda E\psi = E^*\lambda\psi \end{aligned}$$

using the same reasoning as above. It follows that $E = E^*$ and therefore $E \in \mathbb{R}$.

However, this proof is not completely general. As we shall see, the family of Hamiltonians in equation 1.2 lack a real spectrum for $\epsilon < 0$, although the Hamiltonian itself remains $\mathcal{PT}$ symmetric in this regime. We have assumed that the eigenvectors of the Hamiltonian are also eigenvectors of the $\mathcal{PT}$ operator. Because $\mathcal{PT}$ is not a linear operator - the $\mathcal{T}$ operator is antilinear - this is not necessarily the case. We are assured that the eigenvalues of a non-Hermitian Hamiltonian will be real only if the eigenstates corresponding

to these eigenvalues are also $\mathcal{PT}$ eigenstates. The *Hamiltonian* will remain $\mathcal{PT}$-symmetric, but the eigenstates of that Hamiltonian may or may not respect $\mathcal{PT}$ symmetry.

So, to determine if the eigenvalues of a particular $\mathcal{PT}$-symmetric Hamiltonian are real, that is, to say whether there is a real spectrum for a given value of ϵ we must ascertain whether the $\mathcal{PT}$ symmetry of that Hamiltonian is broken or unbroken. It is extremely difficult to determine this in general, and it was not until 2001 in the work of Dorey *et al.* that this was possible. [8] [9].

2.4 Other properties of $\mathcal{PT}$-symmetric Quantum Mechanics

As we have seen, aside from defining the energy eigenvalues for a quantum system, the Hamiltonian also determines the time evolution of states, which must be unitary. By introducing a new inner product on the Hilbert space we can define $\mathcal{PT}$-symmetric theories with unitary time evoluton.

If we proceed in analogy to Hermitian quantum mechanics and define the inner product as

$$\langle\psi|\phi\rangle = \int dx \psi^{\mathcal{PT}}(x)\phi(x)$$

We run into the problem of having negative norm for some states. As the norm of an eigenvector gives us the probability of measuring that eigenvector, this is not acceptable for a physical theory.

This problem is overcome by introducing a new operator called the $\mathcal{C}$ operator, which is named in analogy to the charge conjugation operator of quantum field theory. It expresses a symmetry between the positive and negative norm states.

The norm then becomes the $\mathcal{CPT}$ inner product. That is

$$\langle\psi|\phi\rangle = \int \psi^{\mathcal{CPT}}(x)\phi(x)$$

This is very different from traditional quantum mechanics. We do not need to know the form of the Hamiltonian of a system to take the inner product in that case, but in $\mathcal{PT}$-symmetric quantum mechanics it is nec-

essary to have H to do so. This is because H will tell us which of it's eigenstates has a negative norm, and hence give us the form of the inner product.

In this context we must also modify the condition normally required of an observable that it be a linear, self-adjoint operator $A = A^\dagger$ on the Hilbert space of the system. We replace this with $A^T = \mathcal{CPT}A\mathcal{CPT}$, where A^T denotes the transpose of the operator in some basis. In the $\mathcal{PT}$ symmetric case this guarantees that the expectation value of A for any state is real.

Calculating the $\mathcal{C}$ operator is non-trivial for a given Hamiltonian, It was first calculated by Bender *et al.* [10] using a perturbative approach for the Hamiltonian $H = \frac{1}{2}\hat{p}^2 + \frac{1}{2}\hat{x}^2 + i\epsilon\hat{x}^3$ in which ϵ is treated as a small parameter. Though this approach was quite complicated, it lead to the realisation that $\mathcal{C}$ could be expressed as $e^{Q(x,p)}\mathcal{P}$, where Q is a derivative operator. Using this and a number of algebraic properties of the $\mathcal{C}$ operator, the $\mathcal{C}$ operator has been calculated for a number of Hamiltonians [11] [12] [13] [14].

The concept of $\mathcal{PT}$-symmetry is a subset of a more general set of mathematical theories known as *Pseudo-Hermitian* quantum theories. These theories have arisen in the past as part of attempts to resolve problems that arise when negative-norm states appear in some quantum field theories, such as quantum electrodynamics,s as a result of renormalization. [15] [16] [17] [18] [19].

An operator is pseudo-Hermitian when

$$A^\dagger = OAO$$

Where O is a Hermitian operator which is called the intertwining operator. For ordinary quantum mechanics $O = \mathbb{I}$ [20] [21] [22]. It has been observed that the parity operator may be used as an intertwining operator because it is Hermitian, and for the class of Hamiltonian given by equation 1.2 we see that

$$H^\dagger = \mathcal{P}H\mathcal{P}$$

An overview of pseudo-Hermitian theory is given in [23].

$\mathcal{PT}$-symmetric quantum mechanics can be extended to quantum field the-

ory. The $\hat{x}$ and $\hat{p}$ operators are replaced by the field $\phi(\vec{x}, t)$ and its conjugate $\pi(\vec{x}, t)$. The $\mathcal{P}$ and $\mathcal{T}$ operators behave in an analagous fashion to the quantum mechanical case.

In this context $\mathcal{PT}$-symmetric theory leads to many interesting field theories. A massive scalar field with a $-g\phi^3$ interaction term is interesting because it can be renormalised perturbatively, but such theories are usually thought to have a non-unitary time evolution, and to have an energy spectrum that is unbounded below. With the introduction of the $\mathcal{C}$ operator this is no longer the case. [13] [24]

A $\mathcal{PT}$-symmetric model $-g\phi^4$ theory may be able to describe the dynamics of the Higgs sector as a consequence of broken $\mathcal{P}$ symemtry. This is a consequence of the $\mathcal{PT}$-symmetric boundary conditions, and is not a property of the Hamiltonian of the theory. This parity breaking gives the system a nonzero vacuum expectation value without the need for spontaneous symmetry breaking. [25][26][27][28][29]

The Lee model is an interesting quantum field theory because its mass, wave function and charge maybe be renormalised analytically. However, when the renormalised coupling reaches a certain value, negative norm ghost states appear. It can be shown that with the $\mathcal{C}$ operator these ghost states become normal, positive norm states. [30]

As we shall see, to investigate the eigenvalue spectrum of a Hamiltonian such as those of equation 1.2 it is necessary to extend the problem into the complex plane. This being the case, the natural extension of $\mathcal{PT}$ - symmetric quantum theory to the classical arena is the motion of a particle in the complex plane subject to a $\mathcal{PT}$-symmetric Hamiltonian.

3 Complexified Classical Mechanics

As we outlined in the previous chapter, the $\mathcal{PT}$-symmetric but non Hermitian Hamiltonians such as 1.2 have a real spectrum as long as their $\mathcal{PT}$-symmetry is unbroken.

We can investigate the corresponding classical theory by promoting the real variables x and p to elements of the complex plane, $x, p \in \mathbb{C}$, and examining their behaviour subject to a $\mathcal{PT}$-symmetric Hamiltonian.

This problem has been examined extensively for a number of systems. We pay special attention to the classical theory of the family of Hamiltonians given by equation 1.2. In this chapter we give a brief overview of progress made in this field.

3.1 Hamiltons equations

We may examing the the trajectories of a classical particle subject to

$$H = p^2 + x^2(ix)^\epsilon$$

By solving Hamilton's equations for the system.

$$\frac{dp}{dt} = -\frac{\partial H}{\partial x}$$

$$\frac{dx}{dt} = \frac{\partial H}{\partial p}$$

Which gives us the rates of change of the canonical position and conjugate momenta coordinates with respect to time.

$$\begin{aligned}\frac{dx}{dt} &= \frac{\partial H}{\partial p} \\ &= \frac{\partial}{\partial p}(p^2 + x^2(ix)^\epsilon) \\ &= 2p\end{aligned} \tag{3.1}$$

$$\begin{aligned}\frac{dp}{dt} &= -\frac{\partial H}{\partial x} \\ &= -\frac{\partial}{\partial x}(p^2 + x^2(ix)^\epsilon) \\ &= -\frac{\partial}{\partial x}(-i^2x^2(ix)^\epsilon \\ &= i(2+\epsilon)(ix)^{1+\epsilon}\end{aligned}$$

Noting that equation 3.1 gives us

$$p = \frac{1}{2}\frac{dx}{dt}$$

We can rewrite this pair of equation as

$$\frac{dp}{dt} = \frac{d}{dt}(\frac{1}{2}\frac{dx}{dt})$$

$$\frac{dp}{dt} = \frac{1}{2}\frac{d^2x}{dt^2}$$

$$2\frac{dp}{dt} = \frac{d^2x}{dt^2}$$

$$2i(2+\epsilon)(ix)^{1+\epsilon} = \frac{d^2x}{dt^2}$$

$$\frac{d^2x}{dt^2} = 2(2+\epsilon)i^\epsilon x^{1+\epsilon}$$

This is the *complex force law* for system [30]. It is the complex extension of the regular force law for a particle whose phase space is the real line. To examine the trajectories of these particles we have simply to numerically integrate this system of equations, giving us the behaviour of p and x as a function of t. As the initial conditions on $x(0)$, $p(0)$ may specify points in the complex plane, and as the differential equation is complex, the paths followed by these particles will generally be complex, parameterised by the real variable t.

For most this review attention is restricted to systems which have real values for energy, owing to the fact that in the quantum case we observe

systems which have a real, discrete spectrum.

3.1.1 $\epsilon = 0$

For $\epsilon = 0$ we may choose the initial values to be the turning points ($\frac{dx}{dt} = 0$). In this case we are examining the behaviour of the harmonic oscillator, and the particle will simply oscillate between the two turning points.

All points outside of the turning points and off the real are inside the classically forbidden region. In complexified classical mechanics, however, these regions of the complex plane are valid as initial positions. When we choose a point which lies outside the classically allowed region we observe trajectories which are ellipses with the foci being the turning points. Figure 3.1 illustrates some of these trajectories. All of these paths have the same period as the particle oscillating between the real axis turning points, because we can always deform the contour in the complex plane into the one which lies on the real line without crossing any extra branch points..

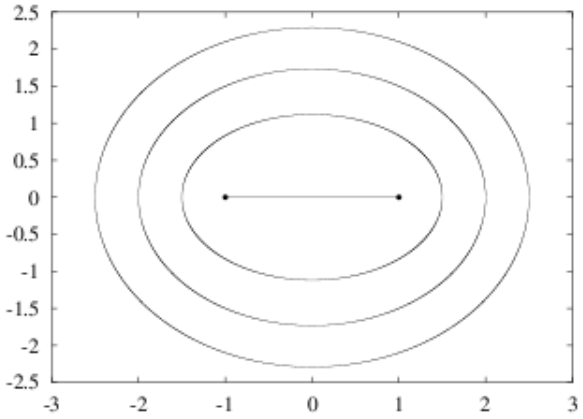

Figure 3.1: Trajectories of a classical particle for $\epsilon = 0$. The particle either oscillates between the pair of turning points or circles them in ellipses with the turning points as the foci. These trajectories all have the same period.

We observe also that these paths are $\mathcal{PT}$-symmetric by which we mean that, if we solve for the path numerically it can be seen that the resulting set of points is symmetric upon reflection across the imaginary axis, an operation which corresponds to $\mathcal{PT}$ symmetry, which is flipping the sign of a complex number and then complex conjugating it.

$$a + ib \rightarrow -a - ib \rightarrow -a + ib$$

3.1.2 $\epsilon > 0$

For $\epsilon = 1$ there are three turning points which solve $ix^3 = 1$. Two of these points exist as a $\mathcal{PT}$ symmetric pair, the third point lies at $x = i$. A particle starting on either of the $\mathcal{PT}$ symmetric pair will oscillate between them, and will follow paths similar to the ellipses in the $\epsilon = 0$ case when this is not the case.

When $x = i$ the particle will move up the imaginary axis to complex infinity in a finite amount of time. A plot of some of these trajectories are illustrated in figure 3.2.

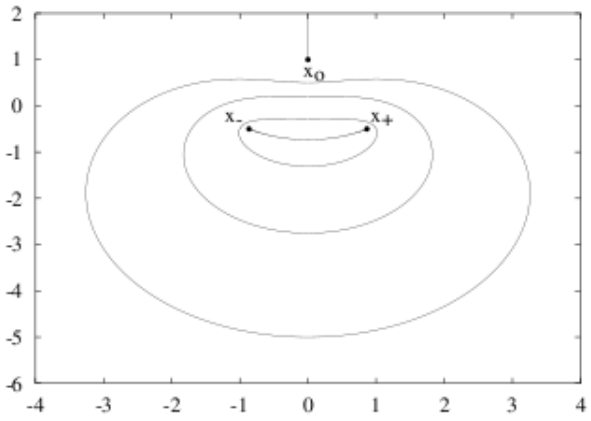

Figure 3.2: Trajectories for a classical particle for $\epsilon = 1$. In this case, there is a set of orbits which oscillates between or around the $\mathcal{PT}$-symmetric pair of turning points. A particle which starts the turning point which lies on the imaginary axis will reach complex infinity in a finite time

For $\epsilon = 2$ there are a pair of orbits which oscillate around the 4 turning points above and below the real axis, in a similar manner to the ellipses which we observer for $\epsilon = 0$. Again, for clarity these orbits are illustrated in figure 3.3.

We note that in general all of the orbits for all $\epsilon > 0$ are closed and $\mathcal{PT}$-symmetric, except for certain integer values of ϵ. For these values there are certain exceptional paths which tend to complex infinity in a finite amount

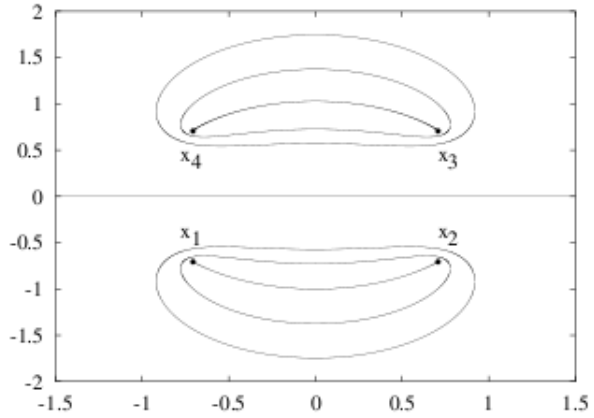

Figure 3.3: For $\epsilon = 2$ there are four turning points. We now have two different types of orbits. One is the set of trajectories which travels directly between or oscillates around the pair of turning points in the top half of the complex plane. There is another set which acts similarly for the pair in the bottom half.

of time, such as the path at the x_0 turning point for $\epsilon = 1$. We also note that in general for noninteger values of ϵ the trajectory of the particle traverses a multisheeted Riemann surface. This is because the function will become multivalued and a branch cut must be introduced to make the function single valued.

3.1.3 $\epsilon < 0$

The case where $\epsilon < 0$ is especially interesting to us, as this corresponds to the quantum case in which the eigenvalues of the Hamiltonian cease to be real.

For $\epsilon = -0.2$ the paths are still $\mathcal{PT}$-symmetric, but they lie on different sheets of the Riemann surface and are open orbits. One branch of the path heads towards complex infinity as $t \to -\infty$,. The other branch tends toward infinity as $t \to \infty$. We observe that in general a negative value of ϵ implies open non-periodic paths, corresponding to the regime in which the eigenvalues for the eigenvalue problem equation1.2 become complex.

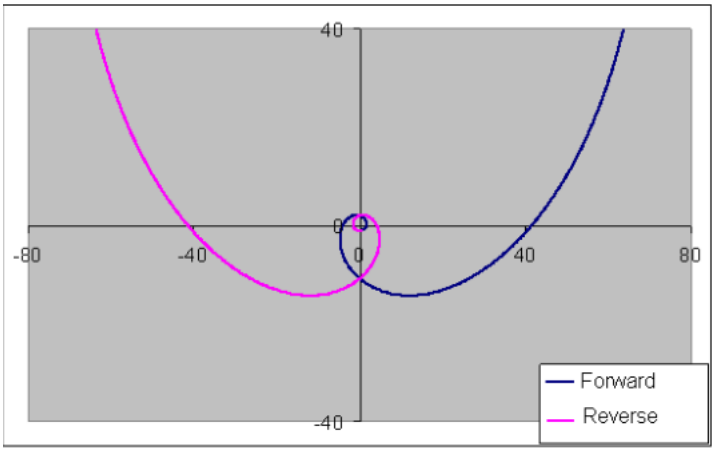

Figure 3.4: A classical orbit for $\epsilon = -0.2$. In this case the oribits are not periodic. They are open and travel towards complex infinity in an infinite time.

3.1.4 Other Systems

The dynamics of various other systems have been investigated in the literature [31] [32]. These include the complex trajectories of a simple pendulum, for which the variable θ is made complex and treated as x, and it's canonical conjugate $\frac{dx}{dt}$ is treated as p. [33]

The study of complexified classical mechanics has lead to the investigation of the behaviour of the complex, $\mathcal{PT}$-symmetric solutions to Euler's differetial equations [34] The beahviour of the kicked rotor and the double pendulum, two chaotic systems, have also been investigated in the $\mathcal{PT}$-symmetric case, [35] as has the Korteweg-de Vries equation [36] [37].

4 Runge-Kutta Methods and Eigenvalue Problems

We would like to investigate the eigenvalue spectrum of the class of Hamiltonians given by the equation

$$\hat{p}^2\psi + \hat{x}^2(i\hat{x})^\epsilon\psi = E\psi$$

In the position space basis we replace $\hat{x}$ for the coordinate variable x and $\hat{p}$ for $-i\frac{d}{dx}$, and we get the linear second-order differential equation

$$-\frac{d^2\psi(x)}{dx^2} + i^\epsilon x^{2+\epsilon}\psi(x) = E\psi(x) \tag{4.1}$$

This equation defines an *eigenvalue problem*. The equation 4.1 only has a non-trivial solution ($\psi \neq 0$) for certain special value of E which are called the eigenvalues [38]. These nontrivial solutions define a set of eigenvalues E_n and their associated eigenfunctions $\psi_n(x)$. When we say we want to investigate the spectrum of a Hamiltonian, we mean that we want to discover these special values of E for which equation 4.1 is satisfied.

To do so, we integrate 4.1 numerically, varying E until the eigenfunctions satisfy a specific condition. This method of discerning the eigenvalue spectrum is called *shooting*. We will detail this method and the Runge-Kutta algorithm used to perform the integration in this chapter.

4.1 Runge Kutta methods

A *differential equation* of order n is one in which the nth derivative of a function of x depends both on the variable x and on the $(n-1)th$ and lower derivatives at y. That is,

$$\frac{d^n y}{dx^n} = f(x, y, \frac{dy}{dx}, \frac{d^2y}{dx^2}, ..., \frac{d^{(n-1)}y}{dx^{(n-1)}})$$

In general it is not always possible to solve such systems of equations analytically. However in the case of first-order differential equations we may arrive at solutions numerically through the application of the *Runge-Kutta methods*, given some suitable initial conditions for a specified value of $x = a$, by evaluating the function $f(x, y)$ a number of times between x_n and x_{n+1} and assigning a suitable weight to each evaluation of the function.

Explicitly, a first-order differential equation is one for which $n = 1$, therefore

$$\frac{dy}{dx} = f(x, y(x))$$

where f is some known function of the variable x and the function y. Given y_0, the value of y at $x = x_0$, we would like to express the difference between y_1, which is the value of y at some known distance from y_0, which is called the *stepsize* of the algorithm, and y_0 as some linear combination of evaluations of f in the interval of x_0 and x_1.

$$y_1 - y_0 = \sum_{i=0}^{n} k_i f_i$$

In this dissertation we will use the Runge-Kutta method of order 4. The *order* of the method refers to how the difference between the numerical approximation of y and the actual value of y at a specified point vary as a function of the stepsize of the algorithm. For brevity, we only present here a derivation of the Runge-Kutta method of order 2. The order 4 method is derive in an analagous fashion. [39]

Observe that we may expand y around a point x_0 as a Taylor series

$$y(x + h) = y(x) + h\frac{dy}{dx} + h^2\frac{d^2y}{dx^2} + \mathcal{O}(h^3)$$

Since we have defined $\frac{dy}{dx}$ to be the function $f(x, y(x))$, we may therefore write

$$y(x + h) = y(x) + hf(x, y(x)) + \frac{h^2}{2}\frac{d^2y}{dx^2} + \mathcal{O}(h^3)$$

We may express $\frac{d^2y}{dy^2}$ as

$$\begin{aligned}\frac{d^2y}{dx^2} &= \frac{d}{dx}\frac{dy}{dx} \\ &= \frac{d}{dx}f(x,y) \\ &= \frac{\partial f}{\partial x} + \frac{\partial f}{\partial y}\frac{\partial y}{\partial x}\end{aligned}$$

So we write the Taylor expansion of y about x as

$$y(x+h) = y(x) + hf(x,y) + \frac{h^2}{2}(\frac{\partial f}{\partial x} + \frac{\partial f}{\partial y}\frac{\partial y}{\partial x}) \tag{4.2}$$

which is

$$y(x+h) = y(x) + Ahf_0 + Bhf_1 \tag{4.3}$$

where

$$f_0 = f(x,y) \qquad f_1 = f(x+Ph, y+Qhf_0)$$

We now solve for A, B, P and Q. First, note that we can exapand f_1 about x, y as follows

$$f(x+Ph, y+Qhf_0) = f(x,y) + hP\frac{\partial f}{\partial x} + hQ\frac{\partial f}{\partial y}f_0 + \mathcal{O}(h^2)$$

Inserting this into equation [4.3]

$$y(x+h) = y(x) + Ahf_0 + Bh\left(f_0 + Ph\frac{\partial f}{\partial x} + Qh\frac{\partial f}{\partial y}f_0\right) + \mathcal{O}(h^3) \tag{4.4}$$

We now match power of h and derivative terms between equations [4.2] and [4.3] to find

$$(A+B)hf_0 = hf_0 \qquad \frac{h^2}{2}\left(\frac{\partial f}{\partial x} + \frac{\partial f}{\partial y}f(x,y)\right) = Bh\left(\frac{\partial f}{\partial x}Ph + \frac{\partial f}{\partial y}Qhf_0\right)$$

Which gives us the system of equations

$$A + B = 1 \qquad PB = \frac{1}{2} \qquad BQ = \frac{1}{2}$$

Taking $A = 0$, $B = 1$ and $P = Q = \frac{1}{2}$. we arrive at the Runge-Kutta method of order 2.

$$y(x+h) = y(x) + hf(x + \frac{h}{2}, y + \frac{h}{2}f(x,y))$$

A similar derivation gives us the Runge-Kutta method of order 4, for which we approximate $y_{n+1} - y_n = \sum_{i=1}^{4} k_i f_i$ This may be expressed as the following algorithm

$$\begin{aligned} k_1 &= f(x_n, y_n) \\ k_2 &= f(x_n + \tfrac{1}{2}h, y_n + \tfrac{1}{2}k_1) \\ k_3 &= f(x_n + \tfrac{1}{2}h, y_n + \tfrac{1}{2}k_2) \\ k_4 &= f(x_n + h, y_n + \tfrac{1}{2}k_3) \end{aligned}$$

$$y_{n+1} = \tfrac{1}{6}(k_1 + 2k_2 + 2k_3 + k_4)$$

We now need a set initial conditions x_0, y_0. Once these are defined we may implement the algorithm iteratively to evaluate the function at an arbitrary value of i. That is, at each step we solve for $y(x_0 + ih)$.

The numerical value of y_i at each step should approximate the actual value of y at this point, which we shall call Y_i, to within an error which varies with the stepsize within the order of $\mathcal{O}(h^4)$, if the method really is an order 4 method. That is, if our algorithm is correct and implemented correctly, we expect that $\sqrt{(y_i - Y_i)^2} < \mathcal{O}(h^4)$.

4.1.1 Testing our algorithm

To ensure that the algorithm we have outlined above is actually accurate to order 4, we will apply it to some differential equation for which analytical solutions can also be derived, and compare the results from the numerical integration to the analytic solutions for various different values of h to ensure that our error scales in the correct manner.

We will take our equation to be

$$u' + 4u = 0$$

we will also specify the value of the function at $x = 0$ to be

$$u(0) = 3$$

having specified this condition we can now solve analytically for u at every

value for x.

We can deduce that $u \propto e^{-4x}$. That is, $u = \alpha e^{-4x}$, where $\alpha \in \mathbb{R}$ is some constant which uniquely determines the equation. We then solve for α by applying the condition at $x = 0$.

$$u(0) = \alpha e^{0} = 3$$

From which we can see that $\alpha = 3$ and the correction solution for u is

$$u(x) = 3e^{-4x}$$

The corresponding problem that we will solve numerically using the Runge-Kutta method is

$$\begin{aligned} u_0 &= 3 \\ x_0 &= 0 \\ u`(x,u) &= -4u \end{aligned}$$

Table 4.1: Error variation with stepsize.

$u(\frac{1}{2})$ - Numerical	Error	Stepsize	# steps
0.406005867620201	1.791036×10^{-8}	0.01	50
0.406005850810721	1.100883×10^{-9}	0.0005	100
0.406005849778072	6.823396×10^{-11}	0.005	200
0.406005849714085	4.246887×10^{-12}	0.00125	400
0.406005849710103	2.648776×10^{-13}	0.000625	800
0.406005849709947	1.084487×10^{-13}	0.0005	1000
0.406005849709855	1.653785×10^{-14}	0.0003125	1600

Table 4.2: Variation in the error of the numerical approximation of $u(\frac{1}{2}$ as the stepsize is varied. The exact value for which is $u(\frac{1}{2}) = 0.406005849709838$

In table 4.2 we numerically integrated this equation from 0 to $\frac{1}{2}$ using a certan value for the stepsize, h. After doing this the value computed from the numerical method was compared to the analytical value and the error was calculated as the absolute value of the difference of the two. We then halved the stepsize iteratively and compared the change in the error for each value of the stepsize.

As it transpired the error scaled much as we would expect. Since we were

halving for each evaluation and as the error ought to be proportional to $\mathcal{O}(h^4)$, we expect the error to be reduced by approximately $\frac{1}{16}$ as we reduce the stepsize by $\frac{1}{2}$. This is pretty much the behaviour we witnessed.

4.2 Second-order ODEs

We begin our discussion of second-order differential equations by noting the definition of a coupled system of differential equations.

A *coupled differential equation* is one in which we have m differential equations of order n. The nth derivative of each function is a function of both the lower derivatives of the function itself as well as a function of the lower derivative of the other differential equations with which it is coupled.

For example, for n = 1 and m = 2 we have two functions which we will call u and v. The first derivative of u and of v are explicitly functions of

$$u' = f(x, u(x), v(x))$$

$$v' = g(x, u(x), v(x))$$

To solve a second order differential equations, in which the highest derivative is n = 2 is specificed as a function of $\frac{dy}{dx}$, y and x, we simply reformulate the problem as a pair of coupled first order differential equations!

Specifically, we take an equation which is specified as

$$y'' = f(y', y, x)$$

and we make the replacement $y' \to a$. This equation then becomes

$$a' = f(a, y, x)$$

$$y' = a$$

which are a pair of coupled first order differential equations. Explicitly, let's rewrite the second-order differential equation

$$y'' = f(y', y, x) = 4y' + 3y + x$$

as a pair of coupled first order differential equations. Replacing $y' \rightarrow a$ this becomes

$$a' = f(a, y, x) = 4a + 3y + x$$

$$y' = g(a, y, x) = a$$

We now simply apply the Runge-Kutta method to this pair of equations. The only difference from the regular case being that we ae integrating two equations, and that the current value of the slope is a function of an extra variable - that is, it is a function of a/y as well as y/a.

And so we arrive at the correct algorithm for numerically integrating a second-order differential equation:

$$\begin{aligned} k_1 &= f(x_n, y_n, y'_n) \\ k_2 &= f(x_n + \tfrac{1}{2}h, y_n + \tfrac{1}{2}k_1) \\ k_3 &= f(x_n + \tfrac{1}{2}h, y_n + \tfrac{1}{2}k_2) \\ k_4 &= f(x_n + h, y_n + \tfrac{1}{2}k_3) \end{aligned}$$

$$\begin{aligned} l_1 &= y'(x_n, y_n) \\ l_2 &= y'(x_n + \tfrac{1}{2}h, y_n + \tfrac{1}{2}k_1) \\ l_3 &= y'(x_n + \tfrac{1}{2}h, y_n + \tfrac{1}{2}k_2) \\ l_4 &= y'(x_n + h, y_n + \tfrac{1}{2}k_3) \end{aligned}$$

$$\begin{aligned} y_{n+1} &= \tfrac{1}{6}(k_1 + 2k_2 + 2k_3 + k_4) \\ y'_{n+1} &= \tfrac{1}{6}(k_1 + 2k_2 + 2k_3 + k_4) \end{aligned}$$

We only need specify the values of a(0), y(0) in order to solve these equations numerically.

4.2.1 Testing Our Algorithm

We will now apply this method to a specific second-order differential equation for which we have an analytical answer.

$$y'' + 4y + 3y = 0$$

with the conditions $y(0) = 1$ and $y'(0) = 0$. Solving the characteristc

equation m^2+4m+3 we get roots of $m=-1,-3$. This gives us the generic solution

$$y(x) = c_1 e^{-x} + c_2 e^{-3x}$$

From the conditions $y(0) = 1 = c_1 + c_2$ and $y'(0) = -c_1 - 3c_2 = 0$ we can solve for c_1 and c_2 given our initial conditions, $c_1 = -\frac{1}{2}$ and $c_2 = \frac{3}{2}$ The exact solutions are then given by

$$y(x) = \frac{3}{2}e^{-x} - \frac{1}{2}e^{-3x}$$
$$y'(x) = -\frac{3}{2}e^{-x} + \frac{3}{2}e^{-3x}$$

We will solve the coupled pair of first-order differential equations

$$\begin{aligned} y' &= a \\ a' &= -4a - 3y \\ y(0) &= 1 \\ a(0) &= 0 \end{aligned}$$

The scaling of the error for y and y' is outlined in tables 4.4 and 4.6.

Table 4.3: Error variation with stepsize.

$y(2)$ - Numerical	Error	Stepsize	# steps
0.216564223679059	1.232192×10^{-2}	0.5	4
0.209087344854927	4.845044×10^{-3}	0.25	8
0.203887092654560	1.189054×10^{-3}	0.125	16
0.200574494975389	3.552083×10^{-4}	0.02	100
0.201760500175768	3.048591×10^{-6}	0.00005	40000
0.201762939018281	6.097483×10^{-7}	0.000001	200000 1

Table 4.4: The variation of the error with the stepsize for y(2) calcualted numerically as pair of coupled first-order differential equations. The analytical expression gives $y(2) = 0.201763548766586$

4.3 The WKB approximation

We see that we can now integrate a second-order differential equation as a coupled pair of first-order differential equations, subject to suitable initial

Table 4.5: Error variation with stepsize for the other case.

$y'(2)$ - Numerical	Error	Stepsize	# steps
-0.170551741168041	1.727943×10^{-2}	0.5	4
-0.188425146005614	9.802548×10^{-3}	0.25	8
-0.193974283966928	4.602296×10^{-3}	0.125	16
-0.198870728955586	4.140676×10^{-4}	0.02	100
-0.199283681351278	1.115239×10^{-6}	0.00005	40000
-0.199284573510217	2.230797×10^{-7}	0.000001	200000 1

Table 4.6: The variation of the error with the stepsize for y'(2) calcualted numerically as pair of coupled first-order differential equations. The analytical expression gives $y'(2) = -0.199284796589920$

conditions on the variables we are integrating. In order to apply this method to the Schrodinger equation we need to derive the correct initial conditions for the problem.

To do this, we appeal to WKB theory. The WKB method in general is applicable to linear differential equations in which the highest derivative of the equation is multiplied by a small parameter, β. This corresponds to problems which exhibit highly oscillatory or exponential decaying behaviour. [38]

$$\beta \frac{d^n y}{dx^n} + a(x) \frac{d^{n-1}}{dx^{n-1}} + ... + k(x) \frac{dy}{dx} + m(x)y = 0 \tag{4.5}$$

We may then assume that the solution to equation 4.5 is

$$y(x) \propto exp(\frac{1}{\delta} \sum_{n=0}^{\infty} \delta^n S_n(x))$$

We may substitute this into the differential equation, cancel out the exponential terms and solve for the different terms in the expansion, δ^n.

Specifically, let us do this for the case of a second order differential equation whose highest derivative is multiplied by the parameter β^2

$$\beta^2 \frac{d^2 y}{dx^2} = Q(x)y \tag{4.6}$$

Plugging in $y(x) = exp(\frac{1}{\delta} \sum_{n=0}^{\infty} \delta^n S_n(x))$, we find

$$\frac{d^2y}{dx^2} = \frac{d}{dx}(\frac{dy}{dx})$$

$$\begin{aligned}\frac{dy}{dx} &= \frac{d}{dx}(exp(\frac{1}{\delta}\sum_{n=0}^{\infty}\delta^n S_n(x))) \\ &= (\frac{1}{\delta}\sum_{n=0}^{\infty}\delta^n \frac{dS_n}{dx}(x))y(x)\end{aligned}$$

Differentiating again and using the product rule

$$\begin{aligned}\frac{d^2y}{dx^2} &= \frac{d}{dx}(\frac{1}{\delta}\sum_{n=0}^{\infty}\delta^n \frac{dS_n}{dx}(x))y(x) + (\frac{1}{\delta}\sum_{n=0}^{\infty}\delta^n \frac{dS_n}{dx}(x))\frac{dy}{dx} \\ &= \frac{1}{\delta}\sum_{n=0}^{\infty}\delta^n \frac{d^2S_n}{dx^2}(x))y(x) + (\frac{1}{\delta}\sum_{n=0}^{\infty}\delta^n \frac{dS_n}{dx}(x))(\frac{1}{\delta}\sum_{n=0}^{\infty}\delta^n \frac{dS_n}{dx}(x))y(x)\end{aligned}$$

Placing this back into [ ] we find

$$\beta^2\left(\frac{1}{\delta}\sum_{n=0}^{\infty}\delta^n S_n'' + \frac{1}{\delta^2}(\sum_{n=0}^{\infty}\delta^n S_n')^2\right)y(x) = Q(x)y(x)$$

From which we can express $Q(x)$ as

$$Q(x) = \beta^2\left(\frac{1}{\delta}\sum_{n=0}^{\infty}\delta^n S_n'' + \frac{1}{\delta^2}(\sum_{n=0}^{\infty}\delta^n S_n')^2\right)$$

Expanding to leading order in δ we get the following explicit expression for $Q(x)$

$$Q(x) = \beta^2\left(\frac{1}{\delta}(S_0'') + \frac{1}{\delta^2}(S_0' + \delta S_1')(S_0' + \delta S_1')\right)$$

We now take the limit of this expression as δ tends to zero

$$Q(x) = \frac{\beta^2}{\delta}S_0'' + \beta^2\frac{{S_0'}^2}{\delta^2} + \frac{2\beta^2}{\delta}S_0'S_1'$$

In the limit $\delta \to 0$ the term $\propto \frac{1}{\delta^2}$ will grow quicker than the other terms as the square of an infinitesimally small number is greater than the small number itself.

So we have an expression of the from of

$$\frac{\beta^2}{\delta^2}S_0'^2 \propto Q(x)$$

As $\frac{\beta^2}{\delta^2}$ is simply a constant number we can just choose some function $S_0(x)$ such that $\frac{\beta^2}{\delta^2}$ in this expression is equal to one, i.e., we just rescale

our original expression giving us the exact expression

$$(\frac{dS_0}{dx})^2 = Q(x)$$

The solution of which can trivially be seen to be

$$S_0(x) = \int_0^x \sqrt{Q(s)}ds$$

This approximation will soon be directly applied to the Schrodinger equation, as it is an equation of the form of 4.6 above, with the function $Q(x)$ equal to the potential term $V(x)$ in the expression for the Hamiltonian.

4.4 The Harmonic Oscillator

Before solving equation 4.1 in the general case of arbitrary ϵ, we will demonstrate how we arrive at the eigenvalue spectrum for the special case $\epsilon = 0$. In this instance the Hamiltonian 4.1 reduces to the harmonic oscillator problem.

$$-\frac{d^2}{dx^2}\psi(x) + (x^2 - E)\psi(x) = 0 \tag{4.7}$$

To perform the integration of equation 4.7, we need to derive the correct initial conditions for the problem. We can do this by appealing to the WKB theory outlined above, and by requiring that the eigenfunctions of the Hamiltonian satisfy certain boundary conditions.

4.4.1 Initial Conditions

Thanks to the WKB approximation we can write the solutions for ψ as

$$\psi(x) \propto e^{\int_0^x \sqrt{V(s)}ds}$$

Performing the integral for $V(s) = s^2$ we find

$$\begin{aligned}\int_0^x \sqrt{V(s)}ds &= \int_0^x \sqrt{(}s^2)ds \\ &= \int_0^x \pm s ds \\ &= \frac{\pm x^2}{2}\end{aligned}$$

Therefore $\psi(x) \propto e^{\pm\frac{x^2}{2}}$. Since we can see from 4.7 that any linear combination of solutions to this equation is also a solution, we can see that if $\psi(x)$ is a solution, then so is $a\psi(x)$. That is, a solution is only a solution up to a multiplicative constant. We are therefore free to assume any value for ψ at our initial position x_0.

If we assume that $\psi(x_0) = a$ it only remains to derive the correct initial condition on $\psi'(x)$. This follows from the condition of square integrability. If the eigenfunctions of our Hamiltonian are not square integrable then they do not define a Hilbert space and we cannot speak of quantum mechanics in that space. To satisfy this condition we assume that $\psi(x) \to 0$ as $|x| \to \infty$. We can deduce from this the correct sign in the exponential term. That is, $\psi(x) \propto e^{\frac{-x^2}{2}}$.

This means that $\psi'(x)$ is given by

$$\frac{d\psi}{dx}(x) \propto \frac{d}{dx} e^{\frac{-x^2}{2}} = -xe^{\frac{-x^2}{2}}$$

This gives us the following set of initial conditions on the eigenfunctions

$$\begin{aligned} \psi(x_0) &= a \\ \psi'(x_0) &= -x_0 a \end{aligned}$$

4.4.2 Shooting conditions

We can now integrate numerically for the wavefunction for different values of E. Each E specifies a different differential equation, whether or not it actually is a valid eigenvalue of the system. So how do we discern eigenvalues from other values? Note that we cannot vary E and try to find soultions which tend to 0 as we increase x. We must start at some positive value for x and integrate *inward* from that point. This is because the solutions of the differential equation are actually a lienar combination of an exponentially growing and an exponentially dying part. If we integrate outwards the value of ψ will always, given enough time, increase, as the integration routine will see each solution as equally valid.

So, to find the eigenvalues, we find some condition that real solutions of the equation ought to satisfy. In this case, we will use our numerical integration routine to obtain these values at the origin. Let's call this property $A_1 = A(E_1)$ and $A_2 = A(E_2)$, where A is evaluated at the origin. We will

integrate inwards and obtain a numerical estimate of this property for two guesses of the correct eigenvalue, E_1 and E_2. We then assume that A is a linear function of E, and using this property we extrapolate an intelligent next guess for the energy as

$$E_{next} = \frac{E_2 A_1 - E_1 A_2}{A_1 - A_2}$$

This is the value of E for which A will be 0 if it were really a linear function of E. It does not matter if it is not in fact a linear function of E (which it almost certainly isn't), it will still converge on the value for E which minimises A in a number of iterations. We then replace one of the old values, E_1 or E_2 with this guess, and iterate this process until we arrive at a value for E for which the function A tends to 0.

A solution to the simple harmonic oscillator satisfies having either even or odd parity. That is, a solution is either

$$\psi(-x) = \psi(x)$$

in which case it is even, or

$$\psi(-x) = -\psi(x)$$

in which case it is odd. We can then reason that in order to satisfy these constraints, either the function itself must be 0 at the origin, or it's first derivative must be 0.

This is easy to justify. If the function is odd then we can see that it must be equal to 0 at the origin, otherwise the function would be discontinuous at that point, which cannot happen as the wavefunction is by definition continuous.

For the case of even parity it is also easy to see. Firstly we note that the derivative of an even function is an odd function.

$$f(x) = f(-x)$$

taking the derivative of both sides and writing $a = -x$ for clarity

$$\frac{df}{dx} = \frac{d}{dx} f(a)$$

and using the chain rule for the right hand side

$$\frac{d}{dx}f(a) = \frac{da}{dx}\frac{df}{da} = -f'(a) = -f'(-x)$$

Therefore

$$f'(-x) = -f'(x)$$

Applying the same reasoning as before, i.e., that quantum mechanics stipulates that the first derivative of the wavefunction must be continuous, we arrive at the conclusion that the value of $f'(x)$ must be 0 at $x = 0$. Figure 4.1 illustrates the situation pictorially.

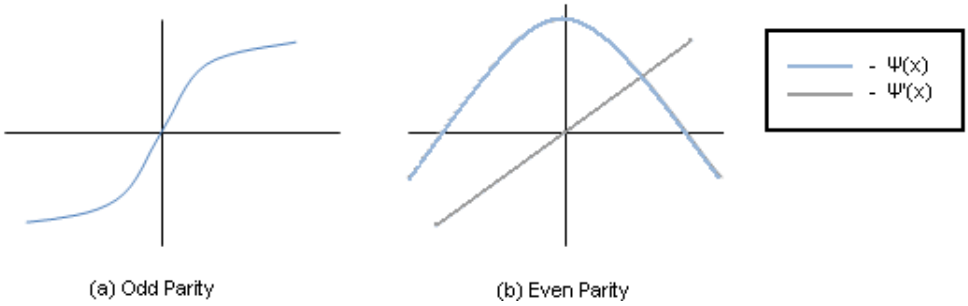

Figure 4.1: The behaviour of odd and even parity harmonic oscillator eigenfunctions at the origin. (a) For the odd parity case, $\psi(0) = 0$ (b) For even parity solutions, $\psi'(0) = 0$ because ψ experiences a turning point at the origin.

4.4.3 Numerical Vs. Analytical

Finally, we give a comparison of the first ten eigenvalue computed numerically versus the analytical expression for the harmonic oscillator eigenvalues, which is given by $E_n = 2n + 1$, in order to give some idea of the accuracy of the shooting algorithm.

Table 4.7: Eigenvalue accuracy.

n	E_n (numerical)	E_n (analytical)	Parity
0	1.0000000000000074942	1.0	EVEN
1	3.0000000000000538176	3.0	ODD
2	5.0000000000003683729	5.0	EVEN
3	7.0000000000010735640	7.0	ODD
4	9.0000000000023283805	9.0	EVEN
5	11.0000000000042862935	11.0	ODD
6	13.0000000000071049763	13.0	EVEN
7	15.0000000000109392703	15.0	ODD
8	17.0000000000159462547	17.0	EVEN
9	19.0000000000222813955	19.0	OD D

5 Classical Spontaneous $\mathcal{PT}$ symmetry breaking

In chapter 3 we summarised the behaviour of complexified classical systems subject to a $\mathcal{PT}$-symmetric Hamiltonian. We found that the orbits are closed $\mathcal{PT}$-symmetric subsets of the complex plane when the solutions obey $\mathcal{PT}$ symmetry, $\epsilon > 0$ for the Hamiltonians in equation 1.2. Conversely, when the $\mathcal{PT}$-symmetry of the solution is broken, the paths in the complex plane are open orbits tending towards infinity, $\epsilon < 0$.

It was first noticed in [40] that the paths taken by a classical particle were highly sensitive to the values of ϵ and $x(0)$, the initial position of the particle. Varying either parameter slightly could give rise to orbits with extremely complicated topologies which visited multiple sheets of the Riemann surface. The period of these closed trajectories was observed to be a wildly fluctuating function of ϵ.

We not that the period depends on the number of pairs of *turning points* enclosed by the orbit, and on the number of times it encloses these pairs. This is because every orbit can be deformed into a similar orbit which connects two turning points and oscillates back and forth between them, rather than one which encircles them.

We note that the turning points are the points where $\frac{dx}{dt} = 0$. Imposing this condition on equation 1.2 and noting that we can always take $E = 1$ as if this were not the case we could simply rescale x and t until it was true. We find that the turning points are given by

$$1 + (ix)^{2+\epsilon} = 0$$

In general for value of $\epsilon \notin \mathcal{Z}$, but for rational ϵ there are a finite number of turning points on the Riemann surface. Following Bender and Darg [41], we will label the turning points as follows

$$x = exp\left(i\pi\frac{4N-\epsilon}{4+2\epsilon}\right)$$

where $N \in \mathbb{Z}$.

The turning points occur in $\mathcal{PT}$ symmetric pairs for values of $N = (-1,0),(-2,1)\ (-3,2)...$ We will label these pairs of points using the integer K, giving us the $\mathcal{PT}$-symmetric pair of turning points $(K,-K-1)$. The $K=0$ pair of turning points represents the pair of turning points which we analytically continue off the real axis.

For $K \neq 0$ the behaviour of the turning points is more complicated, as the trajectory of the particle may now visit many pairs of turning points. In [41] the behaviour of the period of these trajectories was observed for pairs of turning points for which $K \neq 0$. Three regions of behaviour were observed as ϵ was varied for the Kth pair of turning points. As ϵ was increased from 0 the period slowly decreased in a continuous fashion. This behaviour was observed until $\frac{1}{K}$, at which point the period of the trajectory suddenly became a choppy, wildly varying function of ϵ. When the value of ϵ was greater than $4K$ the period began to decrease with increasing ϵ, displaying very similar behaviour to that which was observed in the $< \frac{1}{K}$ region.

The explanation for the choppy variation of the orbit was found [41] to be due to certain special orbits which exhibited broken $\mathcal{PT}$ symmetry. We can see from figure II that there are regions where the period is a small and slowly varying function of ϵ. These regions are bounded by values of ϵ for which the period starts to become very long. Numerical studies indicated that $\epsilon = \frac{p}{q}$ where $p > 0$ is an integer multiple of 4 and q is an odd number, it was observed that the orbits followed by the particle were not $\mathcal{PT}$ -symmetric. This phenomenon has been dubbed *spontaneous* $\mathcal{PT}$ symmetry breaking. An example of one of the non-$\mathcal{PT}$-symmetric orbits which is responsible for this effect is displayed in figure [5.2]. It is generally observed for these orbits that if we start the particle from a specific turning point, it will run into the turning point which is the complex conjugate of the turning point from which its trajectory started, preventing the orbit from being $\mathcal{PT}$-symmetric. The particle then oscillates back and forth between this turning point and its complex conjugate.

For ϵ close to these special, non-$\mathcal{PT}$-symmetric orbits, the turning points of the Hamiltonian will have shifted slightly. When this occurs the particle

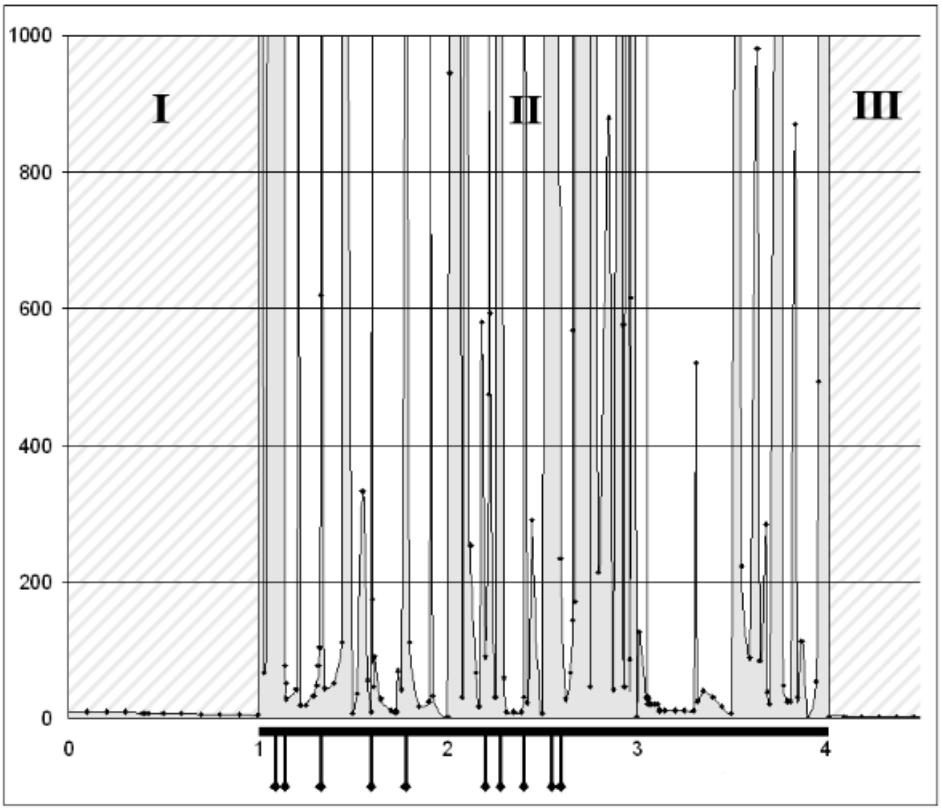

Figure 5.1: Behaviour of period of the trajectory for the K = 1 pair of turning points as a function of ϵ. In region I the period is smoothly varying. In region II it becomes choppy and discontinuous. In region III it returns to the continuous behaviour of region I. Reproduced from [41].

will now just miss the complex conjugate turning point which reflects its trajectory in the special case of $\mathcal{PT}$ symmetry, before embarking on a much longer trajectory in the complex plane before being reflected by a turning point.

Until the discovery of these orbits it was thought that all closed periodic orbits were $\mathcal{PT}$ symmetric. However, we now see that there exist sets of orbits which are closed and periodic but which are not invariant under the $\mathcal{PT}$ operator.

Note that this behaviour occurs only when $K \neq 0$. But many of the numerical investigations of quantum systems carried out to date have been conducted only for the standard $K = 0$ turning points. It is now natural

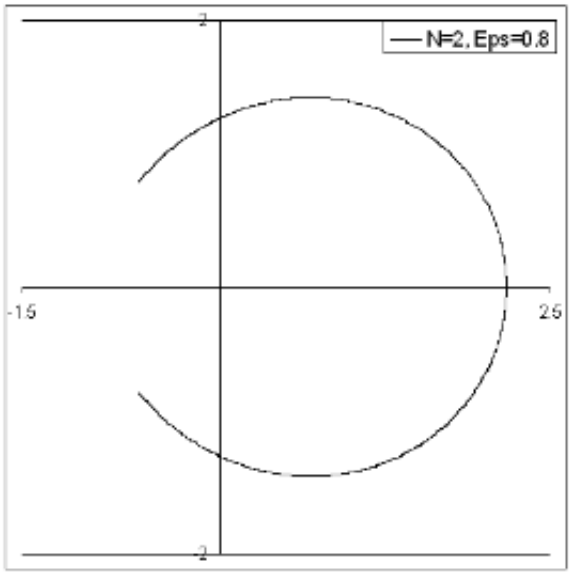

Figure 5.2: A non-$\mathcal{PT}$-symmetric orbit. It can be seen that this orbit is not $\mathcal{PT}$ symmetric, as it is not symmetric upon reflection through the imaginary axis.

to ask whether there is a quantum phenomenon corresponding to this novel classical behaviour.

5.1 Bohr-Sommerfeld Quantization

As some motivation for the possibility of a quantum/classical correspondence, we summarise what is generally known of the relationship between the two regimes for the $\mathcal{PT}$ symmetric case.

We can apply the *Bohr-Sommerfeld* quantization conditions to these contours. The Bohr-Sommerfeld condition takes the classical analysis of the system and demands that the only valid solutions in the quantum scenario are those solutions which are divisible by an integral number of de Broglie wavelengths. That is

$$\oint_C dxp = \oint_C dx\sqrt{E - x^2(ix)^\epsilon}$$

Where C is the contour in the complex plane that defines the orbit of the classical particle. This condition gives the system a set of quantized energy levels indexed by the integer n as

$$E_n = (n + \frac{1}{2})\pi$$

We now have some intuition as to why our Hamiltonians behave the way they do. In chapter 3 we saw that for $\epsilon > 0$ the integration contour for this integral is a well defined closed subset of the complex plane.

However, as illustrated in figure 3.4, when $\epsilon < 0$ the paths the complex particles follow and hence the countours they define for Bohr-Sommerfeld quantization are open paths in the complex plane, along which the classical particle approaches complex infinity in an infinite amount of time. Since the integration contour is not closed for $\epsilon < 0$ it is not possible to perform this integral.

In [42] Bender and Hook constructed pairs of isospectral Hamiltonians, that is, pairs of Hamiltonians having the same eigenvalue spectrum, one of which possesed eigenfunctions that satisfied real differential equations and whose boundary conditions could be defined along the real line. It's corresponding isospectral Hamiltonian satsifed a complex differential equation, with boundary conditions defined in Stokes' wedges in the complex plane.

In the classical limit it was observed for each closed periodic trajectory of one of the Hamiltonians there existed a corresponding closed periodic trajectory for its partner which possesed the same period. This appears to be the classical counterpart of the quantum spectral equivalence. In observing this equivalence it was impotant to note the number of times the particle visited a specific sheet of the Riemann surface. This is because, naively, the periods of these pairs of Hamiltonians may have appeared to be dissimilar, but it was found that the particle may have to traverse the same orbit a number of times on different sheets to revisit its starting point. Once this was taken into account it could be seen that these pairs of Hamiltonians had identical periods.

The general interpretation for this behaviour (see [34]) is that the classical particles are bound in a complex classical atom and cannot run off to infinity. We can see then that only $\mathcal{PT}$-symmetric orbits are physically relevant, those corresponding to the case where the eigenvalues are real. This being the case, we can now turn our attention to the central problem examined as part of this dissertation. As sets of closed, periodic, but non$\mathcal{PT}$ -symmetric solutions have been discovered in the classical scenario, what is

the corresponding behaviour for the quantum system?

6 Numerical Analysis of Eigenvalue Spectra

Before investigating the quantum counterpart of the phenomena outlined in chapter 5, we must extend our Runge-Kutta shooting method so that we can obtain the eigenvalues for a general $\mathcal{PT}$-symmetric Hamiltonian. We will examine the eigenvalue spectra for the Hamiltonians of equation 1.2 for the case $K = 0$, and compare our results to those already present in the literature. We will then briefly summarise the literature documenting other the eigenspectra of other classes of $\mathcal{PT}$-symmetric Hamiltonians.

6.1 The $p^2 + x^2(ix)^\epsilon$ Spectra

We have seen above how to integrate the differential equation 4.7 numerically. To extend these techniques to the more general case we must modify our shooting methods and integration routine. We will see that in order to impose the correct boundary conditions we must make the variable x complex, and as the condition of $\mathcal{P}$ symmetry does not hold in this more general case, we must derive a new shooting condition to distinguish the correct set of eigenvalues E_n. The analytic continuation of eigenvalue problems relies heavily on the work of Bender and Wu on divergent perturbation series [43], [44], and a detailed description of how to analytically continue eigenvalue problems is contained in the paper by Bender and Turbiner [45].

6.1.1 Stokes' wedges

For the harmonic oscillator problem, the condition that $\psi \to 0$ as $|x| \to \infty$ along the real axis guarantees that we have quantized energy levels and that the eigenfuctions of the Hamiltonian are square-integrable. This condition is sufficient as long as $-1 < \epsilon < 2$. For arbitrary real ϵ we must continue the problem into the complex-x plane.

The domain of the integral is redefined from being the real x-axis to a contour in the complex-x plane, with the condition on this contour being that it lies within a wedge of some opening angle in the complex plane. The wedges place a restriction on the argument of $x = re^{i\theta}$ as we tend towards complex infinity. If $\psi(x) = e^{-\int_0^x \sqrt{Q(s)}ds}$, we can express this as $\psi(x) = e^{a+ib} = e^a e^{ib}$. We can only guarantee that $\psi \to 0$ for certain values of the argument of x, as otherwise the value of b will ensure that the asymptotic behaviour of ψ is oscillatory, and thus cannot tend to 0.

If we express this contour as

$$x(t) = r(t)e^{i\theta(t)}$$

Where the variable t parameterises the contour, then we say that $\psi(x) \to 0$ as $r \to \infty$ if $\theta_1 < \theta < \theta_2$ as $t \to \infty$. If this is the case we can then impose the boundary condition that ψ approaches zero at the end points of the contour. [4] This situation is depcited in figure [6.1].

For the Hamiltonians we are examining the centres of the Stokes' wedges inside which we can guarantee the wavefunction will tend to 0 are given by

$$\theta_{left} = -\pi + \frac{\epsilon}{\epsilon+4}\frac{\pi}{2} \qquad \theta_{right} = -\frac{\epsilon}{\epsilon+4}\frac{\pi}{2}$$

Each of which has an opening angle of $\frac{2\pi}{\epsilon+4}$.

As ϵ increases these wedges rotate downward from the simple harmonic oscillator wedges which encompass the real line at $\epsilon = 0$, As ϵ tends to infinity, the opening angle of the wedge's tends to 0 and the Stokes' wedges lie along the negative imaginary axis [46]. The eigenvalues are real and positive and rise with increasing ϵ. In $\epsilon \to \infty$ limit the eigenvalue problem has no solutions, as the solution contour can be pushed off to infinity. In this limit it has been observed that the eigenvalues all become infinite.

6.1.2 Shooting conditions

The condition that $\psi(x) = 0$ or $\psi'(x) = 0$, which we used to discern even and odd parity solutions for the simple harmonic oscillator only holds when we have symmetry under the $\mathcal{P}$ operator. We'll need something more general for the other differential equations we will be examining. Fortunately there is also a condition that we can impose on more general solutions to

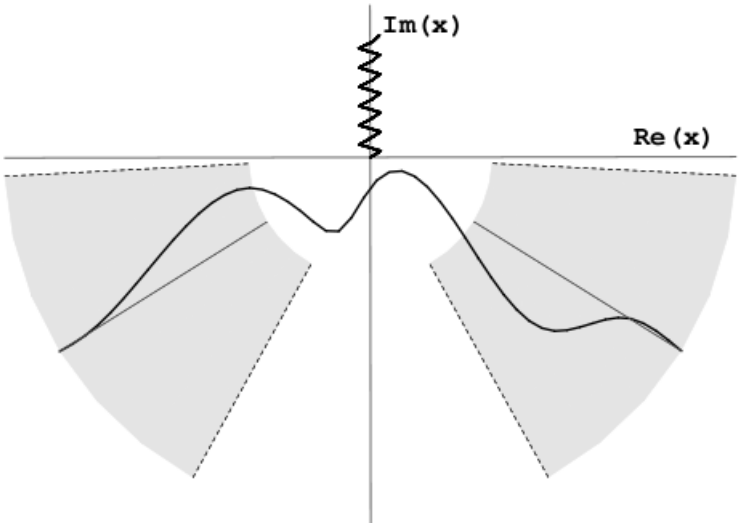

Figure 6.1: Stokes' wedges. As we increase ϵ above 0, the pair of Stokes' wedges rotate downards towards the negative imaginary axis, their opening angle decreasing as ϵ increases.

an eigenvalue equation. In the more general case we simply ask that the wavefunction be *continuous*.

To ensure this we will integrate in from the left, and from the right, and ensure that the resulting values of the wavefunction are continuous at the origin. That is:

$$\psi_L(x) - \psi_R(x) = 0$$

However, there is a problem with this technique: any linear combination of solutions to the Schrodinger equation is also a solution. Therefore multiple of a solution is also a solution. Since we'll be starting at two totally different values of x and integrating into the origin, we have no way of guaranteeing that the values of ψ when integrated inward from the left and from the right are not multilpied by two totally different constants.

However, we can overcome this problem by noting that if $\psi(x)$ is a solution and we multiply it by c, then we have $c\psi(x)$. Taking the first derivative

$$\frac{cd\psi}{dx} = c\frac{d\psi}{dx}$$

so we can just divide out the constants. Our shooting condition becomes

$$\frac{\psi_L'(x)}{\psi_L(x)} - \frac{\psi_R'(x)}{\psi_R(x)} = 0$$

We now repeat the procedure we used for the harmonic oscillator, taking two initial guesses for E, integrating from the left, and the right, into the origin for these values, and using the supposition that the difference between these values is a linear function of E to extrapolate our next guess for energy.

6.1.3 Integrating in the complex plane

So we see that to solve the eigenvalue equation 1.2 for $\epsilon > 2$ it is necessary to continue the eigenvalue problem off the real axis and into the lower half of the complex plane, with the condition that the eigenfunctions we are examining tend to 0 as long as they lie asymptotically within a pair of wedges in the complex plane, which lie at some angle and have some specified opening angle.

Given this we can then guarantee that the function tends to 0 as the distance from the origin tends towards ∞. This is necessary to ensure that our theory be square-integrable and so we can interpret it in a probabalistic manner.

However, we must be careful about performing a Runge-Kutta integration in the complex plane. The integration scheme only works if we have one independent variable. Naively, we have two in the complex case. However, we will simply rewrite the position variable as $x = re^{i\theta}$.

In this case we will integrate along r and the factors involving θ will simply become some phase factors multiplying the paired couple of complex equations (four paired real equations).

$$\frac{d^2\psi}{dx^2} = \frac{d^2r}{dx^2}\frac{d^2\psi}{dr^2}$$

$$\frac{dr}{dx} = \frac{1}{\frac{dx}{dr}}$$

$$\frac{dx}{dr} = \frac{d}{dr}(re^{i\theta}) = e^{i\theta}$$

Therefore

$$\frac{d^2\psi}{dx^2} = e^{-2i\theta}\frac{d^2\psi}{dr^2}$$

The full differential equation becomes

$$-e^{2i\theta}\frac{d^2\psi}{dr^2} + (r^2e^{2i\theta})(ri)^\epsilon e^{\epsilon i\theta} = E\psi$$

More concisely, this is

$$-e^{2i\theta}\frac{d^2\psi}{dr^2} + i^\epsilon r^{2+\epsilon} e^{(2+\epsilon)i\theta} = E\psi$$

Due to the fact that we are integrating in the real variable r, we must note how this affects our shooting condition. The shooting condition is given by

$$\frac{\psi_L'(x)}{\psi_L(x)} - \frac{\psi_R'(x)}{\psi_R(x)} = 0$$

Where $\psi'(x)$ refers to $\frac{d\psi}{dx}$. However, we are integrating in r, and when we recast the second-order complex differential equation as a pair of first-order complex different equations, we will be solving for $\frac{d\psi}{dr}$, *not* $\frac{d\psi}{dx}$. However, we can express $\psi'(x)$ in terms of $\frac{d\psi}{dr}$ using the chain rule.

$$\frac{d\psi}{dx} = \frac{dr}{dx}\frac{d\psi}{dr} = e^{-i\theta}\frac{d\psi}{dr}$$

Evidently, the correct shooting condition in terms of our integration variables will become

$$e^{-i\theta_{left}}\frac{\psi_L'(x)}{\psi_L(x)} - e^{-i\theta_{right}}\frac{\psi_R'(x)}{\psi_R(x)} = 0$$

Where we note that $\theta_{left} \neq \theta_{right}$ because they lie within two different Stokes wedges, and by $\psi'(x)$ we now mean $\frac{d\psi}{dr}$.

6.1.4 Accuracy

We now have a method for investigating the spectra of the class of Hamiltonians given by equation 1.2.

Before we apply it we would like to ascertain the accuracy to which our eigenvalues can be trusted. We checked the accuracy by varying both the stepsize h and the initial value of the position, x_0. Decreasing the former and increasing the latter should give us more accurate estimations of the eigenvalues. We can then infer that we may trust our numerical calculation only as far as the last decimal point which still agrees with the more accurate

estimation.

It was found that the accuracy decreased as n for the eigenvalue we were finding increased. This is expected because higher eigenvalues correspond to solutions to the equation which oscillate more rapidly as a function of x. It can be seen that the $n = 9$ eigenvalue is approximtely 3 to 4 decimal places less accurate than the $n = 0$ eigenvalue.

Some comparisons of the same eigenvalue calculated with different step-sizes and initial x are contained in table 6.1.

Table 6.1: Eigenvalue accuracy.

n	h	$\|x_0\|$	E	ϵ
0	0.0005	5	1.15626707198811263643	1
0	0.0005	10	1.15626707198810993395	1
0	0.0005	20	1.15626707198809715576	1
0	0.001	10	1.15626707198810399653	1
0	0.0001	10	1.15626707198811369559	1
0	0.00001	10	1.15626707198820403847	1
9	0.0005	5	37.469825359625047612 32	1
9	0.0005	10	37.469825361652339679 17	1
9	0.0005	20	37.469825361559638231 96	1
9	0.01	10	37.470011365980301708 27	1
9	0.001	10	37.469825379236726521 64	1
9	0.0001	10	37.469825360527167269 07	1

6.1.5 Results

Figure [6.2] shows a portion of the eigenvalue spectrum which we calculated using our Runge-Kutta integration method. It can be seen that this work reproduces the spectra calculated in the literature, a plot of which is shown for comparison in figure [6.3].

As ϵ increases from 0 the eigenvalues increased and grew further far apart. This behaviour persists for as far as could be examined using the Runge-Kutta scheme implemented for this system, which is approximately $\epsilon = 5.5$. Above this value, the magnitude of ψ grew too high as we integrated to be stored to *long double* accuracy.

When we investigated $\epsilon < 0$ the eigenvalues follow the same pattern as they do for $\epsilon > 0$. That is, as we decrease from 0 the spectra grew closer

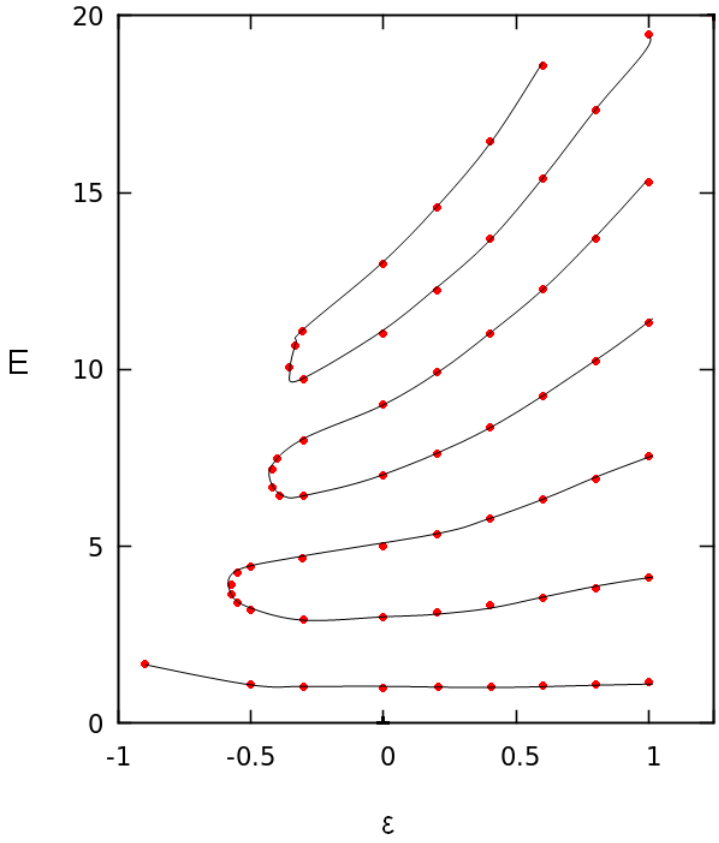

Figure 6.2: Portion of the eigenvalue spectrum for the $\hat{p}^2 + \hat{x}^2(ix)^\epsilon$ Hamiltonian

together. This behaviour persists until around $\epsilon = 0.75$. At this point the distinct real eigenvalues grow closer together, becoming the same eigenvalue, before disappearing from the spectrum. This effect is indicative of the fact that these pairs of eigenvalues are moving off the real line. At these points, they split into complex conjugate pairs. .

6.2 Eigenvalue Spectra of other Hamiltonians

Finally, we present a brief overview of the studies that have been conducted into the behaviour of the Eigenvalue spectra for some other classes of Hamiltonians. The Hamiltonians (1.2) we have studied in this dissertation are a subset of a much larger class of Hamiltonians which are invariant under the $\mathcal{PT}$ operator. Some insight into the behaviour of their spectra may

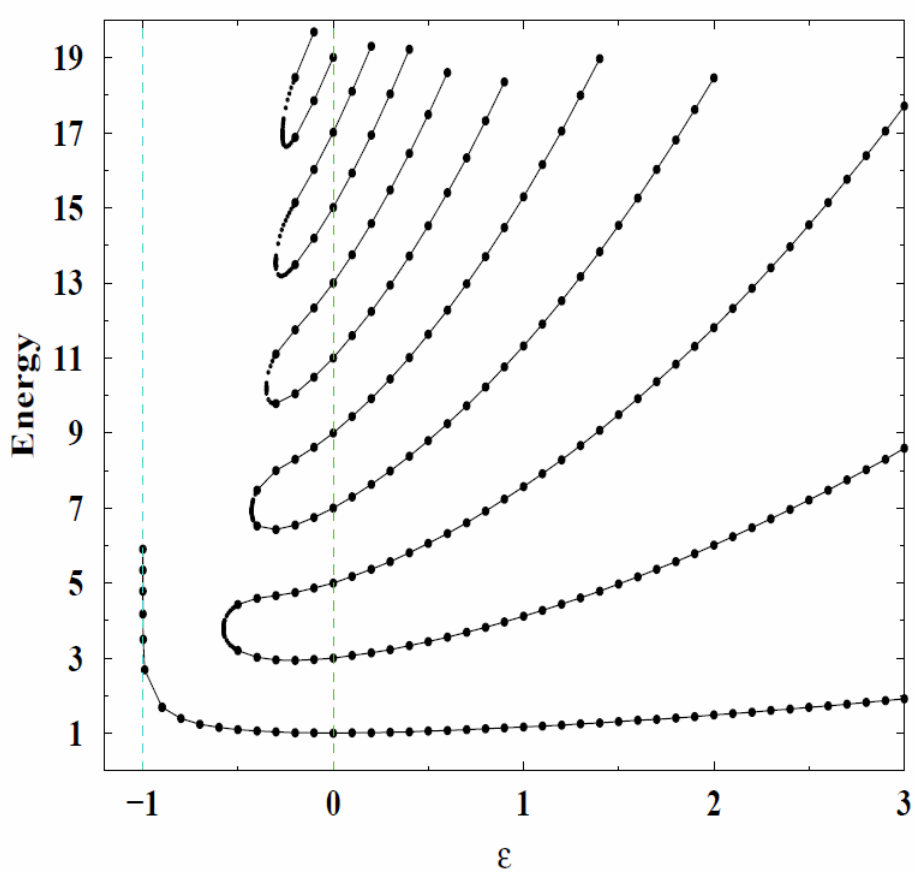

Figure 6.3: A larger portion of the spectrum of the eigenvalue spectrum for the $\hat{p}^2 + \hat{x}^2(ix)^\epsilon$ Hamiltonian. Provided for comparison with 6.2. Reproduced from [30].

prove insightful for understanding the case we investigated as part of this dissertation.

6.2.1 The $\hat{p}^2 + x^4(ix)^\epsilon$ spectra

The wider class of Hamiltonians $H = p^2 + x^{2K}(ix)^\epsilon$ were studied by Bender, Boettcher and Meisinger in [46]. For the case $K = 1$ this becomes the class of Hamiltonians we studied computationally in this dissertation. However, when $K \neq 1$ there are a number of interesting effects which have been observed and which are relevant to the content of this dissertation.

In this more general case, the Schrodinger equation in the coordinate-space basis becomes

$$-\psi''(x) + (x^{2K}(ix)^{\epsilon} - E)\psi(x) = 0$$

The centres of the Stokes' wedges for this problem are now given by

$$\theta_{right} = -\frac{\epsilon\pi}{4K + 2\epsilon + 4} \qquad \theta_{left} = -\pi + \frac{\epsilon\pi}{4K + 2\epsilon + 4}$$

which are again $\mathcal{PT}$-symmetric.

The eigenvalue spectrum for $\hat{p}^2 + x^4(ix)^{\epsilon}$ as calculated in [46] is displayed in figure 5. For $\epsilon > 0$ the beaviour of the eigenvalues is the same as in the case we have studied. That is, the eigenvalues increase monotonically with ϵ. When ϵ ranges from -1 to 0 a finite of the eigenvalues are real, along with an infinite set of complex conjugate pairs of eigenvalues due to $\mathcal{PT}$ symmetry breaking.

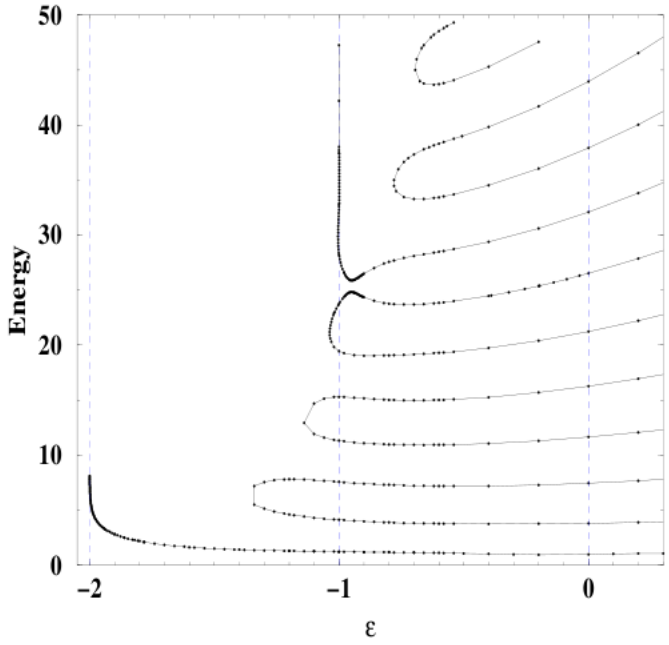

Figure 6.4: Eigenvalue spectrum of the Hamiltonian $\hat{p}^2 + x^4(ix)^{\epsilon}$. Reproduced from [46]

However, at $\epsilon = -1$ the spectrum emerges from the complex plane and is entirely real. After this point, the eigenvalues return to the complex plane and continue to pinch off in pairs until there is only one eigenvalue left as ϵ approaches -2. As the lowest eigenvalue approaches -2 it begins to

diverge logarthimically. Once $\epsilon < -2$ the Hamiltonians no longer exhibit a spectrum with any real eigenvalues.

6.2.2 The $\hat{p}^2 + x^6(ix)^\epsilon$ spectra

When $K = 2$ these Hamiltonians become $\hat{p}^2 + x^6(ix)^\epsilon$. Their spectra as a function of ϵ is displayed in figure [6.5], which is also reproduce from [46] The spectrum is similar to the case detailed in the previous subsection, but there is now an extra phase transition.

For $\epsilon \geq 0$ the spectra grow and diverge with ϵ. As ϵ decreases below 0 the eigenvalues again pinch off and enter the complex plane, the number of real values decreasing in pairs as this happens. At $\epsilon = -1$ and $\epsilon = -2$ we again see an entirely real spectrum briefly emerging from the complex plane. As ϵ decreases below -2 the lowest eigenvalue again diverges logarithmically as $\epsilon \to -3$. For $\epsilon \leq -3$ there are no real eigenvalues.

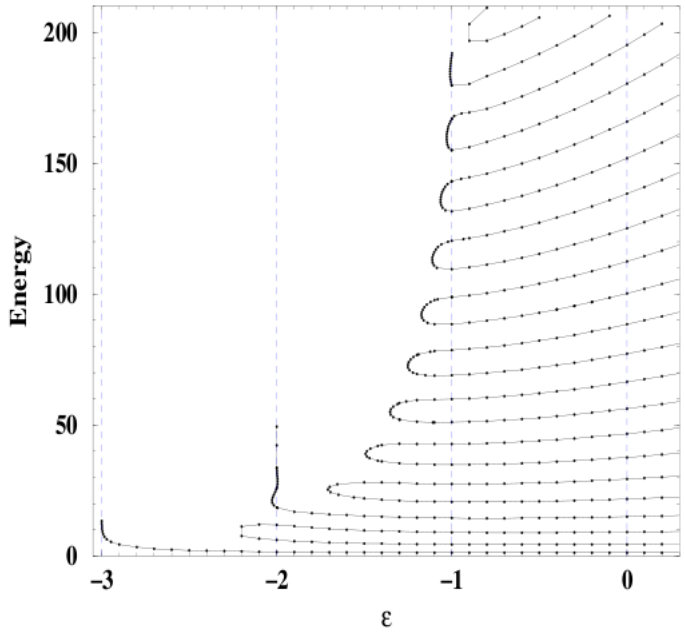

Figure 6.5: Eigenvalue spectrum of the Hamiltonian $\hat{p}^2 + x^6(ix)^\epsilon$. Reproduced from [46].

7 Quantum Spontaneous $\mathcal{PT}$ Symmetry Breaking

We are now ready to present the results of this dissertation. We remind you that the problem we have set out to investigate is to discover the quantum counterpart of the classical phenomena observed by Bender and Darg [41] described in chapter 5. We will see that there is a compelling correspondence between the behaviour of the classical and quantum systems. We reiterate that the form of this family of Hamiltonians is

$$H = \hat{p}^2 + \hat{x}^2(ix)^\epsilon \tag{7.1}$$

7.1 Numerical evaluation of eigenvalue spectrum at unconventional turning points

To examine the behaviour of these system we desire to investigate the eigenvalue spectrum of the Hamiltonians (7.1) for the unconventional turning points indexed by the variable K. The program constructed to examine the spectrum is capable of probing the eigenspectrum of (7.1) up to $\epsilon \sim 5.5$. The exponential behaviour of the wavefunction means that ψ grows prohibitively large when we try to integrate for ϵ above this value.

As the region of unusual behaviour is given by $\frac{1}{K} < \epsilon < 4K$, we only expect to be able to fully examine the behaviour for $K = 1$. A partial examination of the behaviour for the $K = 2$ case was also undertaken and is summarised below.

In the quantum case the turning points correspond to the points where the behaviour of the eigenfunctions transitions from being oscillatory to dying off exponentially. Associated to each turning point in the classical scenario is a Stokes wedge inside which, for the quantum problem, the function $\psi(x)$ for the differential equation 1.2 may be taken to tend to 0 asymptotically.

We examined the eigenspectrum inside these Stokes wedges for various value of ϵ. We note that although the eigenvalues E_n obtained here may not be numerically precise for higher values of n, they do give an accurate qualitative picture of the behaviour of the eigenvalues.

7.2 Spontenous $\mathcal{PT}$ symmetry breaking for the $K = 1$ pair of turning points

For the $K = 1$ turning point the behaviour is detailed in figure [7.1]

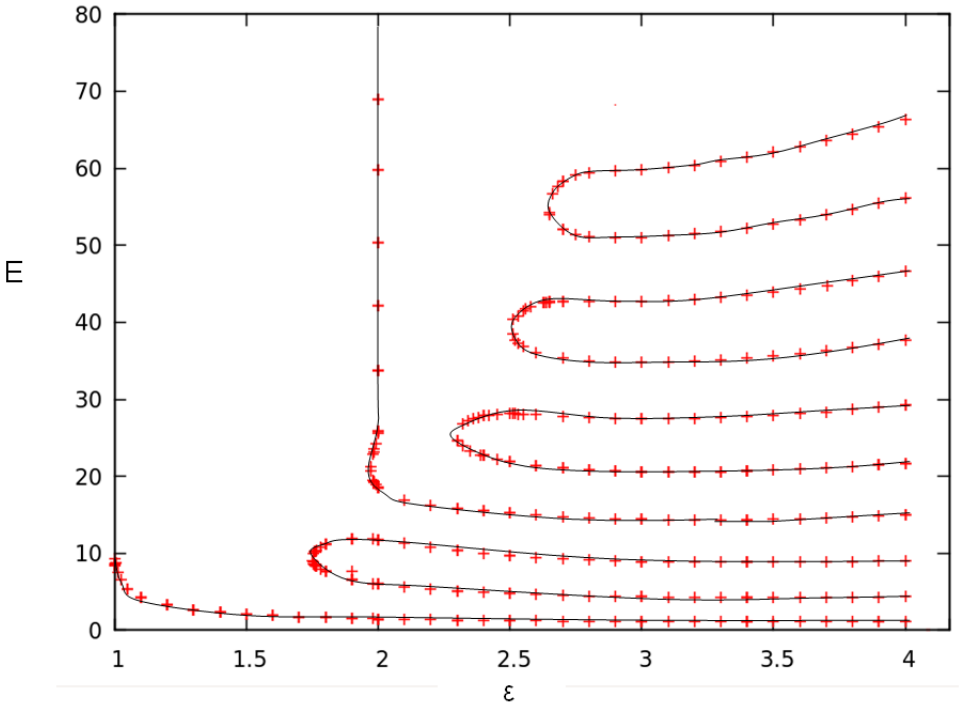

Figure 7.1: The eigenvalue spectrum of the $\hat{p}^2 + \hat{x}^2(ix)^\epsilon$ Hamiltonian for the $K = 1$ turning points.

We note that the behaviour is qualitatively similar to the behaviour of the family of Hamiltonians $p^2 + x^{2K}(ix)^\epsilon$. We observe that the lowest eigenvalue diverges logarithmically as ϵ approaches 1. Above this we observe that the eigenvalues generally pinch off in pairs and enter the complex plane, except for $\epsilon = 2$, at which we point we observe the eigenspectrum briefly emerging from the complex plane and becoming real. This is a phase transition as it represents the brief reemergence of $\mathcal{PT}$-symmetry for this value of ϵ.

For $\epsilon = 3$ it was observed that we could generally find eigenvalues of very high n. For values close to this such as $\epsilon = 2.95, 3.05$, we did not observe eigenvalues of comparable energy. We conjecture that this implies that the eigenvalue spectrum is again briefly real for $\epsilon = 3$. Above this value we believe that the spectrum continues to disappear into the complex plane. We did not detail this behaviour as it occurs at very high value for E, at which our program is no longer of reliable accuracy.

For $\epsilon > 4$ we seem to observe an entirely real spectrum, the eigenvalues become gradually becoming larger and growing apart from one another.

7.3 Spontenous $\mathcal{PT}$ symmetry breaking for the $K = 2$ pair of turning points

Figure 7.2 depicts the behaviour of the eigenspectrum for the $K = 2$ pair of turning points. Again, this behaviour is similar to the family of Hamiltonians $\hat{p}^2 + \hat{x}^{2K}(ix)^\epsilon$. The lowest eigenvalue diverges logarithmically as ϵ approaches 3. For $\epsilon < 5.5$ we observe eigenvalues disppearing into the complex plane in much the same manner as we do for the $K = 1$ case. However, at $\epsilon = 5$ and $\epsilon = 4$ we find that the eigenvalue spectrum again emerges from the complex plane to be briefly real.

It is interesting that we observe two transitions in this case. It may be the case that there is the appearance of real eigenvaluse for every integer value of ϵ between $\frac{1}{K}$ and K. We can only speculate this is the case, as it was not possible to investigate the $K = 1$ spectrum to sufficiently high values of E, nor was it possible to investigate the $K = 2$ spectra for $\epsilon > 5.5$, both of which may have shed more light on the exact behaviour of the phase transitions for these Hamiltonians.

We note that we could not discern any special behaviour of the eigenspectrum at either turning point for the $\epsilon = \frac{p}{q}$, with p a multiple of 4, q odd. It may be the case that this spontaneous breaking for certain value of ϵ manifests itself as a general breakdown in the $\mathcal{PT}$ symmetry of the corresponding quantum eigenspectrum.

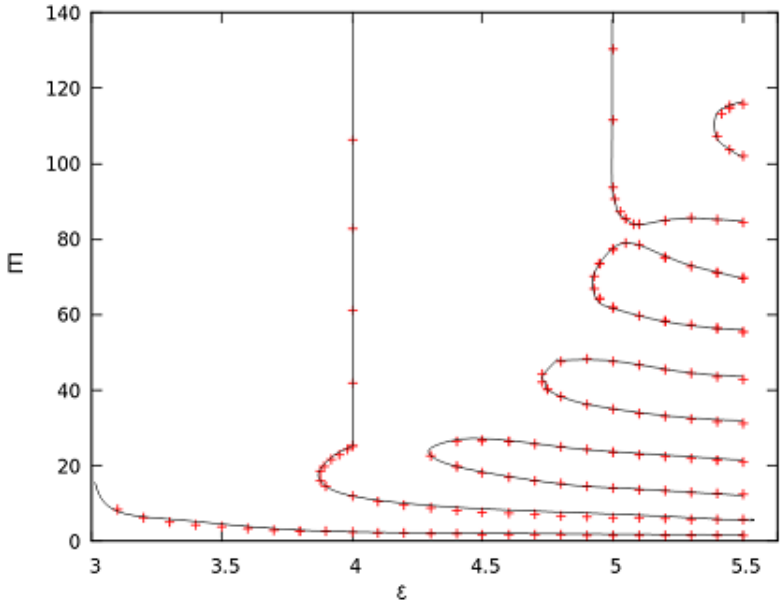

Figure 7.2: The eigenvalue spectrum of the $\hat{p}^2 + \hat{x}^2(ix)^\epsilon$ Hamiltonian for the $K = 2$ turning points.

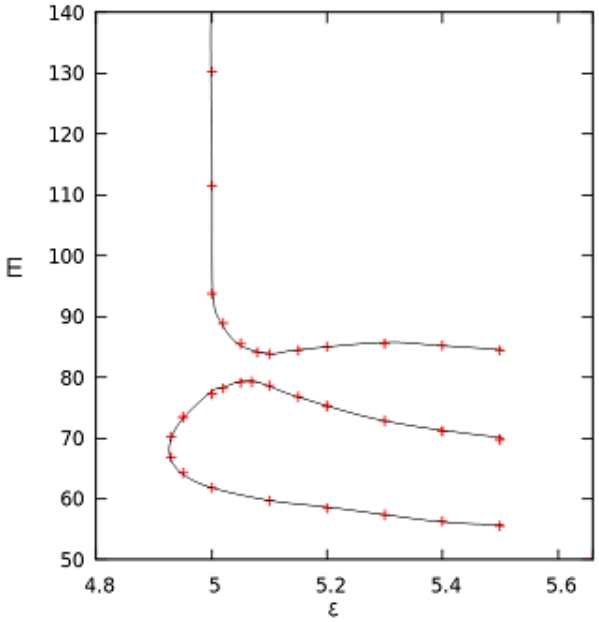

Figure 7.3: A closer view of the eigenvalue spectrum of the $\hat{p}^2 + \hat{x}^2(ix)^\epsilon$ Hamiltonian for the $K = 1$ turning points, for ϵ between 4.8 and 5.6. This figure illustrates the temporary reemergence of the eigenvalues from the complex plane.

8 Conclusions

In this dissertation we have discussed the phenomenon of spontaneous $\mathcal{PT}$-symmetry breaking for the family of Hamiltonians (1.2). We have examined the spectra of the corresponding eigenvalue problem, motivated by the correspondence between classical and quantum systems. We have seen that this motivation has proven to be justified. We have observed an unforseen set of behaviours for the class of Hamiltonians (1.2). For the $K \neq 0$ turning points we observe numerous phase changes for the eigenstates of these Hamiltonians, in the disappearance into and reemergence from the complex plane of the eigenvalues. It may be speculated that these changes in phase are in some way analagous to the breaking of $\mathcal{PT}$ symmetry for certain special values of ϵ in the classical case.

It is undoubtedly the case that further numerical work in this area could lead to very interesting results. More complete surveys of the eigenspectra for $K = 1$ and $K = 2$, for higher values of ϵ and E may result in the discovery of further interesting phenomeona. In particular, it would be interesting to see if there is any correspondence between the behaviour of the eigenvalues for the special rational values of ϵ which give rise to closed, periodic classical orbits which do not exhibit $\mathcal{PT}$-symmetry. Although these spectra were examined for these values of ϵ as part of this dissertation, we could not discern any special beahviour, but more intense numerical work may reveal an interesting correspondence for those values.

We also note that it may be of interest to examine the classical trajectories of the $H = \hat{p}^2 + \hat{x}^{2K}(ix)^\epsilon$ Hamiltonians in the regions which exhibit similar quantum behaviour to the Hamiltonians studied here at the $K = 1, 2$ turning points. It may be the case that there is a similar choppy behaviour of the period of these trajectories for those values of ϵ, representing the presence of closed, broken $\mathcal{PT}$ orbits.

A C Program Implementing First Order Runge-Kutta Integration

```
#include <stdio.h>
#include <math.h>

long double u_exact(long double x);
long double u_prime(long double x, long double u);

int main(void)
{
 long double k1, k2, k3, k4;
 long double h = 0.0003125;
 long double x = 0.0, u = 3.0;
 int i = 0;

 while(i < 1600)
 {
  k1 = h * u_prime (x, u);
  k2 = h * u_prime (x + h*0.5, u + k1*0.5);
  k3 = h * u_prime (x + h*0.5, u + k2*0.5);
  k4 = h * u_prime (x + h, u + k3);

  u += (k1 + k2 + k2 + k3 + k3 + k4)/6.0;

  x += h;
  i++;
 }

 printf("x : %Lf\n", x);
```

```
 printf("u_exact_:_%.15Lf\n", u_exact(x));
 printf("u_numerical_:_%.15Lf\n", u);
 printf("error_:_%Le\n", fabsl(u_exact(x) - u));

 return 0;
}

long double u_exact(long double x)
{
 return (3.0 * expl(-4.0 * x));
}

long double u_prime(long double x, long double u)
{
 return (-4.0 * u);
}
```

B C Program Implementing Second Order Runge-Kutta Integration

```
#include <stdio.h>
#include <math.h>

long double a_prime(long double x, long double y, long double a);

int main(void)
{
 long double k1, k2, k3, k4;
 long double l1, l2, l3, l4;
 long double h = 0.02;
 long double x = 0.0, y = 1.0, a = 0.0;
 int i = 0;
 long double y_exact;
 long double a_exact;

 while(i < 100)
 {
  k1 = h * a_prime (x, y, a);
  l1 = h * a;
  k2 = h * a_prime (x + h*0.5, y + l1*0.5, a + k1*0.5);
  l2 = h * (a + h*0.5*k1);
  k3 = h * a_prime (x + h*0.5, y + l2*0.5, a + k2*0.5);
  l3 = h * (a + h*0.5*k2);
  k4 = h * a_prime (x + h, y + l3, a + k3);
  l4 = h * (a + h*k3);
```

```
  a += (k1 + k2 + k2 + k3 + k3 + k4)/6.0;
  y += (l1 + l2 + l2 + l3 + l3 + l4)/6.0;

  x += h;
  i++;
 }

 printf("x : %.15Lf\n", x);
 y_exact = (3.0/2.0)*expl(-x) - (1.0/2.0)*expl(-3.0*x);
 printf("y :%.15Lf\n", y_exact);
 printf("y numerical: %.15Lf\n", y);
 printf("Error: %Le\n\n",fabsl(y - y_exact));

 a_exact = -(3.0/2.0)*expl(-x) + 3.0/2.0*expl(-3.0*x);
 printf("y':%.15Lf\n", a_exact);
 printf("y' numerical: %.15Lf\n", a);
 printf("Error: %Le\n\n", fabsl(a - a_exact));

 return 0;
}

long double a_prime(long double x, long double y, long double a)
{
 return (-4.0 * a - 3.0 * y);
}
```

C C Program Implementing a Shooting Algorithm to Solve Eigenvalue Differential Equations

```
#include <stdio.h>
#include <math.h>
#include <complex.h>

#define ldc long double complex
#define pi 3.14159265
#define epsilon 0.0

void rk_integrate (ldc x0, ldc *y, ldc *z, long double h,
long double E, long double theta, FILE *output);
ldc F(long double r, long double theta, ldc psi, ldc psiprime,
long double E);
ldc G(long double r, long double theta, ldc psi, ldc psiprime,
long double E);
long double shoot (long double E1, long double E2,
long double A1, long double A2);

int main (void)
{
 long double E1 = 17.5, E2 = 18.0, tempE;
 long double three = 3.0;
 long double stepsize = 0.0005;
 long double theta_left, theta_right;
```

```
ldc psi1_left, psiprime1_left;
ldc psi1_right, psiprime1_right;
ldc psi2_left, psiprime2_left;
ldc psi2_right, psiprime2_right;
ldc psi1_diff, psi2_diff;
ldc x_left, x_right;

int i, loop;

FILE *output

x_right = 10.0 * cexpl(I * pi * ((4.0*1.0 - epsilon)/
      (4.0 + 2.0*epsilon)));
x_left =  10.0 * cexpl(I * pi * ((4.0*-2.0 - epsilon)/
      (4.0 + 2.0*epsilon)));

theta_right = cargl(x_right);
theta_left = cargl(x_left);

loop = (int) x_right/stepsize;
loop++;

output = fopen("output", "w");

psi1_right = 1.0;
psiprime1_right = -cpowl(I, epsilon)
      *cpowl(x_right, (2.0 + epsilon))*psi1_right;
psi2_right = 1.0;
psiprime2_right = -cpowl(I, epsilon)
      *cpowl(x_right, (2.0 + epsilon))*psi2_right;

psi1_left = 1.0;
psiprime1_left = -cpowl(I, epsilon)
      *cpowl(x_left, (2.0 + epsilon))*psi1_left;
psi2_left = 1.0;
psiprime2_left = -cpowl(I, epsilon)
```

```
        *cpowl(x_left, (2.0 + epsilon))*psi2_left;

for (i = 0; i < 40; i++)
{
 rk_integrate (x_right, &psi1_right,
 &psiprime1_right, -stepsize, E1, theta_right, output);
 rk_integrate (x_right, &psi2_right,
 &psiprime2_right, -stepsize, E2, theta_right, output);
 rk_integrate (x_left, &psi1_left,
 &psiprime1_left, -stepsize, E1, theta_left, output);
 rk_integrate (x_left, &psi2_left,
 &psiprime2_left, -stepsize, E2, theta_left, output);

 psi1_diff =  cexpl(-I*theta_left)  *
 (psiprime1_left/psi1_left);
 psi1_diff -= cexpl(-I*theta_right) *
 (psiprime1_right/psi1_right);
 psi2_diff =  cexpl(-I*theta_left)  *
 (psiprime2_left/psi2_left);
 psi2_diff -= cexpl(-I*theta_right) *
 (psiprime2_right/psi2_right);

 printf("%d\t\t%.10Lf\t\t%.10Lf\n", i+1, E1, E2);

 if(!isnan(E1))
 {
  tempE = E1;
  E1 = shoot(E1, E2, cabsl(psi1_diff), cabsl(psi2_diff));
  E2 = tempE;
 }

 else
 {
  printf("%.20Lf\n", E2);
  return 0;
 }
```

```
  psi1_right = 1.0;
  psiprime1_right = -cpowl(I, epsilon)
  *cpowl(x_right, (2.0 + epsilon))*psi1_right;
  psi2_right = 1.0;
  psiprime2_right = -cpowl(I, epsilon)
  *cpowl(x_right, (2.0 + epsilon))*psi2_right;

  psi1_left = 1.0;
  psiprime1_left = -cpowl(I, epsilon)
  *cpowl(x_left, (2.0 + epsilon))*psi1_left;
  psi2_left = 1.0;
  psiprime2_left = -cpowl(I, epsilon)
  *cpowl(x_left, (2.0 + epsilon))*psi2_left;
 }

 printf("%.20Lf\n", E1);

 return 0;
}

void rk_integrate (ldc x0, ldc *y, ldc *z, long double h,
long double E, long double theta, FILE *output)
{
 ldc k1, k2, k3, k4;
 ldc l1, l2, l3, l4;
 ldc psi, psiprime;
 ldc x;
 long double r;

 int loop;

 r = cabsl(x0);

 psi = *y; psiprime = *z;
```

```
 for(loop = 0; loop < 20000; loop++)
 {
  k1 = h * F(r, theta, psi, psiprime,  E);
  l1 = h * G(r, theta, psi, psiprime,  E);

  k2 = h * F(r + h*0.5, theta, psi + k1*0.5,
  psiprime + l1*0.5, E);
  l2 = h * G(r + h*0.5, theta, psi + k1*0.5,
  psiprime + l1*0.5, E);

  k3 = h * F(r + h*0.5, theta, psi + k2*0.5,
  psiprime + l2*0.5, E);
  l3 = h * G(r + h*0.5, theta, psi + k2*0.5,
  psiprime + l2*0.5, E);

  k4 = h * F(r + h, theta, psi + k3,
  psiprime + l3, E);
  l4 = h * G(r + h, theta, psi + k3,
  psiprime + l3, E);

  psi += (k1 + k2 + k2 + k3 + k3 + k4)/6.0;
  psiprime += (l1 + l2 + l2 + l3 + l3 + l4)/6.0;
  r += h;
 }

 *y = psi;
 *z = psiprime;
}

ldc F(long double r, long double theta, ldc psi, ldc psiprime,
  long double E)
{
 return psiprime;
}

ldc G(long double r, long double theta, ldc psi, ldc psiprime,
```

```
  long double E)
{
 ldc retval;
 ldc x;

 x = r*cexpl(I*theta);

 retval = (cpowl(x,2.0)*cpowl(I*x, epsilon) - E)*psi;
 retval = retval*cexpl(2.0*I*theta);

 return retval;
}


long double shoot (long double E1, long double E2,
long double A1, long double A2)
{
 long double E3;

 E3 = (E2*A1 - E1*A2)/(A1–A2);

 return E3;
}
```

Bibliography

[1] M. Fisher, Phys. Rev. Lett. **40**, 1610 (1978).

[2] J. Cardy, Phys. Rev. Lett. **54**, 1354 (1985).

[3] J. Cardy and G. Mussardo, Phys. Lett. B. **225**, 275 (1989).

[4] C. Bender and S. Boettcher, Phys Rev. Lett. **80**, 5243 (1998).

[5] C. M. Bender, Contemp. Phys. **46**, 277 (2005).

[6] D. Griffiths, *Introduction to Quantum Mechanics* .

[7] J. Sakurai, *Modern Quantum Mechanics* .

[8] P. Dorey, C. Dunning, and R. Tateo, J. Phys A: Math. Gen. **34**, 5679 (2001).

[9] P. Dorey, C. Dunning, and R. Tateo, Czech J. Phys **54**, 35 (2004).

[10] C. M. Bender, P. N. Meisinger, and Q. Wang, J. Phys. A.: Math Gen **36**, 1973 (2003).

[11] C. M. Bender, G. V. Dunne, P. N. Meisinger, and M. Simsek, Phys. Lett. A. **281**, 311 (2001).

[12] C. M. Bender, J. Brod, A. Refig, and M. E. Reuter, J. Phys. A: Math. Gen. **37**, 10139 (2004).

[13] C. M. Bender, D. C. Brody, and H. F. Jones, Phys. Rev. Lett. **93**, 251601 (2004).

[14] C. M. Bender, D. C. Brody, and H. F. Jones, Phys. Rev. D. **70**, 025001 (2004).

[15] W. Pauli, Rev. Mod. Phys **15**, 175 (1943).

[16] S. Gupta, Phys. Rev. **77**, 294 (1950).

[17] K. Bleuler, Helv. Phys. Act. **23**, 567 (1950).

[18] E. Sudarshan, Phys. Rev. **123**, 2183 (1961).

[19] T. Lee and G. Wick, Nucl. Phys. B **9**, 209 (1969).

[20] A. Mostafazadeh, J. Math. Phys. **43**, 205 (2002).

[21] A. Mostafazadeh, J. Math. Phys **43**, 2814, 3944, and 6343 (2002).

[22] A. Mostafazadeh, Nucl. Phys. B **640**, 419 , timestamp = 2009.09.13 (2002).

[23] A. Mostafazadeh, http://arxiv.org/abs/0810.5643 (2008).

[24] C. M. Bender, S. F. Brandt, J.-H. Chen, and Q. Wang, Phys. Rev. D **71**, 065010 (2005).

[25] C. M. Bender, K. A. Milton, and V. M. Savage, Phys. Rev. D. **62**, 85001 (2000).

[26] K. Symanzik, Springer Tracts Mod. Phys. **57**, 222 (1971).

[27] F. Kleefeld, J. Phys. A: Math. Gen. **39**, L9 (2006).

[28] P. M. C. M. Bender and H. Yang, Phys. Rev. D **63**, 45001 (2001).

[29] J. M. H. F. Jones and R. J. Rivers, Phys. Rev. D **74**, 125022 (2006).

[30] C. M. Bender, Rep. Prog. Phys. **70**, 947 (2007).

[31] A. Nanayakkara, Czech. J. Phys. **54**, 101 (2004).

[32] A. Nanayakkara, J. Phys. A: Math. Gen. **37**, 4321 (2004).

[33] C. M. Bender, D. D. Holm, and D. W. Hook, J.Phys. A **40** (2007).

[34] C. M. Bender, D. D. Holm, and D. W. Hook, J. Phys. A. - Math Theor **40**, F793 (2007).

[35] C. M. Bender, J. Feinberg, D. W. Hook, and D. J. Weir, http://arxiv.org/abs/0809.1975 (2008).

[36] C. M. Bender, D. C. Brody, J.-H. Chen, and E. Furlan, J. Phys. A: Math. Theor. (2007).

[37] A. Fring, arXiv:math-ph/0701036] .

[38] C. M. Bender and S. A. Orzsag, *Advanced Mathematical Methods for Scientists and Engineers* (Springer, 1999).

[39] Press and Flannery, *Numerical Recipes in C: The Art of Scientific Computing* (CUP, 1992).

[40] C. Bender, J. H. Chen, D. Darg, and K. Milton, J. Phys A: Math. Gen **37**, 4321 (2004).

[41] C. M. Bender and D. W. Darg, J. Math. Phys **48** (2007).

[42] C. M. Bender and D. W. Hook, J. Phys. A: Math. Theor. **41**, 244005 (2008).

[43] C. Bender and T. Wu, Phys. Rev. Lett. **21**, 406 (1968).

[44] C. Bender and T. Wu, Phys. Rev. **184**, 1231 (1969).

[45] C. Bender and A. Turbiner, Phys. Lett. A. **173**, 442 (1993).

[46] C. Bender, S. Boettcher, and P. Meisinger, J. Math. Phys. **40**, 2201 (1999).